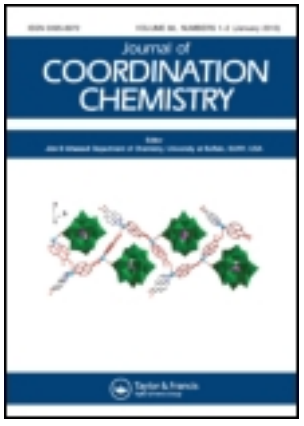

Journal of Coordination Chemistry
Publication details, including instructions for authors and subscription information:
http://www.tandfonline.com/loi/gcoo20

Quinoxaline-based Schiff base transition metal complexes: review

Chellaian Justin Dhanaraj [a], Jijo Johnson [a], Jeyasekaran Joseph [b] & Raphael Selwin Joseyphus [c]

[a] Department of Chemistry, University College of Engineering Nagercoil, Konam, India

[b] Department of Chemistry, Noorul Islam Centre for Higher Education, Kumaracoil, India

[c] Department of Chemistry, St. John's College, Kollam, India

Accepted author version posted online: 07 Mar 2013.Published online: 15 Apr 2013.

To cite this article: Chellaian Justin Dhanaraj, Jijo Johnson, Jeyasekaran Joseph & Raphael Selwin Joseyphus (2013) Quinoxaline-based Schiff base transition metal complexes: review, Journal of Coordination Chemistry, 66:8, 1416-1450, DOI: 10.1080/00958972.2013.782008

To link to this article: http://dx.doi.org/10.1080/00958972.2013.782008

Journal of Coordination Chemistry, 2013
Vol. 66, No. 8, 1416–1450, http://dx.doi.org/10.1080/00958972.2013.782008

Quinoxaline-based Schiff base transition metal complexes: review

CHELLAIAN JUSTIN DHANARAJ*†, JIJO JOHNSON†, JEYASEKARAN JOSEPH‡ and RAPHAEL SELWIN JOSEYPHUS§

†Department of Chemistry, University College of Engineering Nagercoil, Konam, India
‡Department of Chemistry, Noorul Islam Centre for Higher Education, Kumaracoil, India
§Department of Chemistry, St. John's College, Kollam, India

(*Received 7 June 2012; in final form 30 January 2013*)

The literature survey highlights spectra and biological activity of transition metal complexes derived from Schiff bases of quinoxaline. The extensive studies of synthesis, spectral, structural characterization, and biological activities of the metal complexes with heterocyclic Schiff bases of quinoxaline are reviewed.

Keywords: Quinoxaline; Schiff base; Metal complexes; Heterocyclic; Biological activities

1. Introduction

Among complexing ligands, Schiff bases have special interest. Schiff bases, named after Hugo Schiff [1], are formed by condensation of primary amine with an active carbonyl compound. They have an azomethine group –RC=NR,' where R and R' are alkyl, cycloalkyl, aryl or heterocyclic group. Schiff bases with an additional donor close to the imino nitrogen form stable chelates with metal ions. Schiff base metal complexes have been extensively studied for biological applications, such as antimicrobial [2–4], insecticidal [5], anti-HIV [6], antitumor [7], and *in vitro* cytotoxic activities [8]. Many Schiff base metal complexes show excellent catalytic activities in Jacobsen–Katsuki epoxidation [9, 10], oxidation [11], reduction [12], and polymerization reaction [13]. They also serve as photoactive materials [14], electroluminescent materials [15], and non-linear optical materials [16].

2. Importance of heterocyclic ligands

Heterocyclic compounds are important due to their biological and catalytic activities. Many pharmaceutical compounds are characterized by the presence of five-, six- or seven-membered rings containing hetero atoms, behaving as antimalarial, anti-inflammatory,

*Corresponding author. Email: justindhanaraj@yahoo.co.in

analgesic, anticancer, antitumor and antihypertensive agents. Metal complexes of heterocyclic ligands are also used as catalysts [17].

3. Importance of quinoxaline metal complexes

Quinoxaline, also called a benzopyrazine, is a heterocyclic compound containing a benzene ring and a pyrazine ring. Quinoxalines are isomeric with cinnolines, phthalazines, and quinazolines. Studies on synthesis of quinoxaline-based Schiff base complexes have considerable importance because of their interesting chemical and biological properties. Quinoxaline derivatives are widely distributed in nature and have a variety of biological applications [18–31]. Quinoxalines are also important in material science, as magnetic materials [32], organic light emitting diodes [33, 34] and non-linear materials [35].

4. Quinoxaline-based Schiff base ligands

Quinoxaline-based Schiff bases were synthesized and characterized by several workers. Ammar *et al.* [36] reported the synthesis of some Schiff bases from 6-benzoyl-3-amino-2-imino-2,3-dihydrothiazolo[4,5-b]quinoxaline (**1**) (figure 1).

Varghese *et al.* reported [37] the synthesis and crystal structure of N,N′-bis[(E)-quinoxalin-2-ylmethylidene]ethane-1,2-diamine (**2**) (figure 2). The Schiff base was prepared by condensation of quinoxaline-2-carboxaldehyde and ethylenediamine.

The synthesis and crystal structure of two bis-azomethines derived from quinoxaline-2-carboxaldehyde were reported [38]. The crystal structures of the Schiff bases, N,N′-bis [(E)-quinoxalin-2-ylmethylidene]propane-1,3-diamine (**3**) and N,N′-bis[(E)-quinoxalin-2-ylmethylidene]butane-1,4-diamine (**4**) (figure 3), revealed that conformations of the crystal structures were stabilized by aromatic π–π stacking interactions.

A bis-azomethine Schiff base synthesized by condensation of 3-hydroxyquinoxaline-2-carboxaldehyde and 2,3-diaminomaleonitrile (**5**) was characterized by IR, ^{1}H and ^{13}C NMR, HPLC, cyclic voltammetry, thermogravimetry-differential thermal analysis (TG-DTA), and DSC studies. The studies revealed that the Schiff base exists in two major tautomeric forms, i.e. minor enol (**5**a) and major keto (**5**b) forms (scheme 1) [39].

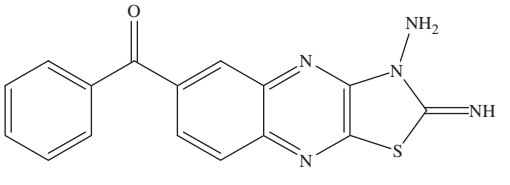

Figure 1. Structure of 6-benzoyl-3-amino-2-imino-2,3-dihydrothiazolo[4,5-b]quinoxaline (**1**).

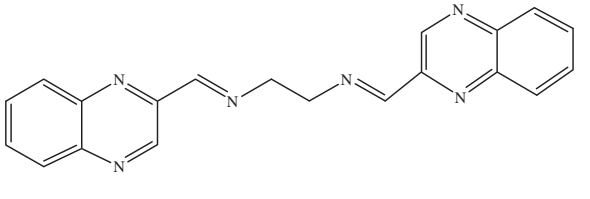

Figure 2. N,N′-bis[(E)-quinoxalin-2-ylmethylidene]ethane-1,2-diamine (**2**).

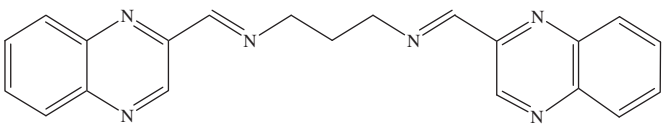

(**3**)

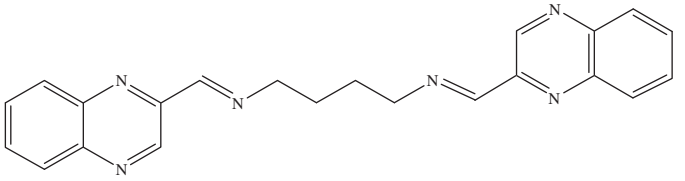

(**4**)

Figure 3. Structure of N,N′-bis[(E)-quinoxalin-2-ylmethylidene]propane-1,3-diamine (**3**) and N,N′-bis[(E)-quinoxalin-2-ylmethylidene]butane-1,4-diamine (**4**).

Leeju *et al.* [40] reported the synthesis and crystal structure of N-[(E)-quinoxalin-2-ylmethylidene]-1H-indazole-5-amine (**6**) (figure 4). In the crystal, weak intermolecular N–H…N hydrogen bond links the molecule into zigzag chains extending in the [0 0 1] direction. The crystal packing also exhibits π–π interactions.

Ratnadeep and Kumar reported [41–43] synthesis and characterization of a series of Schiff bases of quinoxaline-2(1H)-one (**7**a–j) (scheme 2). The synthesized Schiff bases were screened for their anti-inflammatory, anticonvulsant, and antimicrobial activities.

The synthesis and crystal structure of Schiff bases derived from quinoxaline-2-carboxaldehyde with (1S,2S)-(−)-1,2-diaminocyclohexane (**8**) and 1,1′-binaphthyl-2,2′-diamine (**9**) were reported (scheme 3) [44].

Achutha *et al.* [45] synthesized quinoxaline-incorporated Schiff bases by condensation of 2-[(3-methylquinoxalin-2yl)oxy]acetohydrazide with indole-3-carboxaldehyde (**10**a), furfuraldehyde (**10**b), 5-(4-nitrophenyl)-2-furfuraldehyde (**10**c) and substituted benzaldehydes (**10**d) (scheme 4), under conventional and microwave irradiation methods. The microwave method was remarkably successful with higher yields and less reaction time compared to conventional heating method. All the synthesized compounds were characterized by IR, ^{1}H NMR, and mass spectral data; the compounds were evaluated for antitubercular and anti-inflammatory activities.

4.1. *X-ray crystallography of quinoxaline-based Schiff bases*

The crystal structure of **2** has been reported [37]. In the molecule, the central C–C bond lies on a crystallographic inversion center. The quinoxaline ring is nearly planar, with a maximum deviation of 0.021(2) Å from the mean plane. The crystal structure is stabilized by intermolecular C–H…N interactions, leading to formation of a layer-like structure.

Schiff bases **3** and **4** [38] crystallize the monoclinic crystal system. Molecular conformations of the crystal structures are stabilized by aromatic π–π stacking. In the crystal structure of **6**, the mean planes of quinoxaline and indazole fragments form dihedral intermolecular N–H…N hydrogen bonds. The crystal packing also exhibits π–π interactions [40].

5. Quinoxaline-based Schiff base transition metal complexes

Schiff base (QCG) (**11**) and its Fe(III), Co(II), Ni(II), and Cu(II) complexes (**11**a) (figure 5) were synthesized by template method and characterized [46]. Thermal decompo-

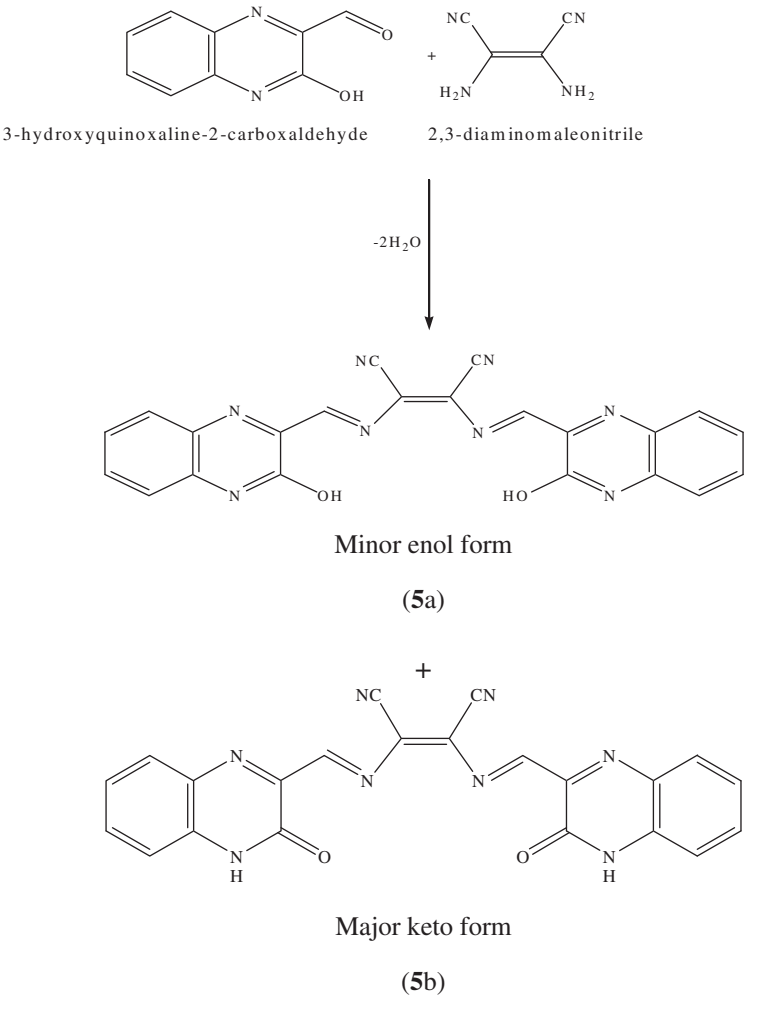

Scheme 1. Synthetic route of **5**.

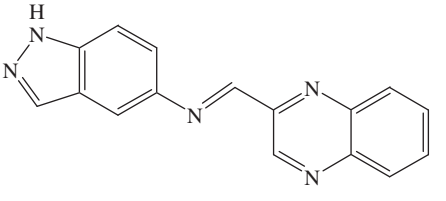

Figure 4. Structure of N-[(E)-quinoxalin-2-ylmethylidene]-1H-indazole-5-amine (**6**).

sition kinetics of Fe(III), Co(II), Ni(II), and Cu(II) complexes of the same ligand were reported [47].

A new Schiff base derived from quinoxaline-2-carboxaldehyde and 2-aminocyclopent-1-ene-1-dithiocarboxylic acid (**12**) and its Fe(III) (**12**a), Co(II), Ni(II), and Cu(II) complexes

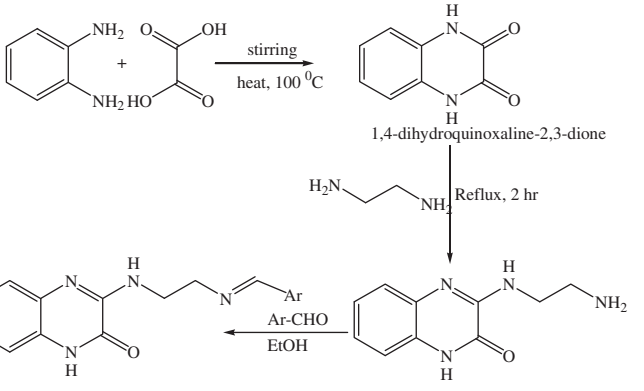

where Ar=C_6H_5CHO (**7**a), Ar=3NO_2-C_6H_4CHO (**7**b), Ar=2NO_2-C_6H_4CHO (**7**c), Ar=2OH-C_6H_4CHO (**7**d), Ar=CH_3O-C_6H_4CHO (**7**e), Ar=$C_6H_5CH_2CH{=}CHCHO$ (**7**f), Ar=3Cl-C_6H_4CHO (**7**g), Ar=$(CH_3)_2N$-C_6H_4CHO (**7**h), Ar=3,4-Cl-C_6H_3CHO (**7**i) and Ar=1$OHC_{12}H_8CHO$ (**7**j).

Scheme 2. Synthetic route of Schiff bases of quinoxaline-2(1H)-one (**7**a–j).

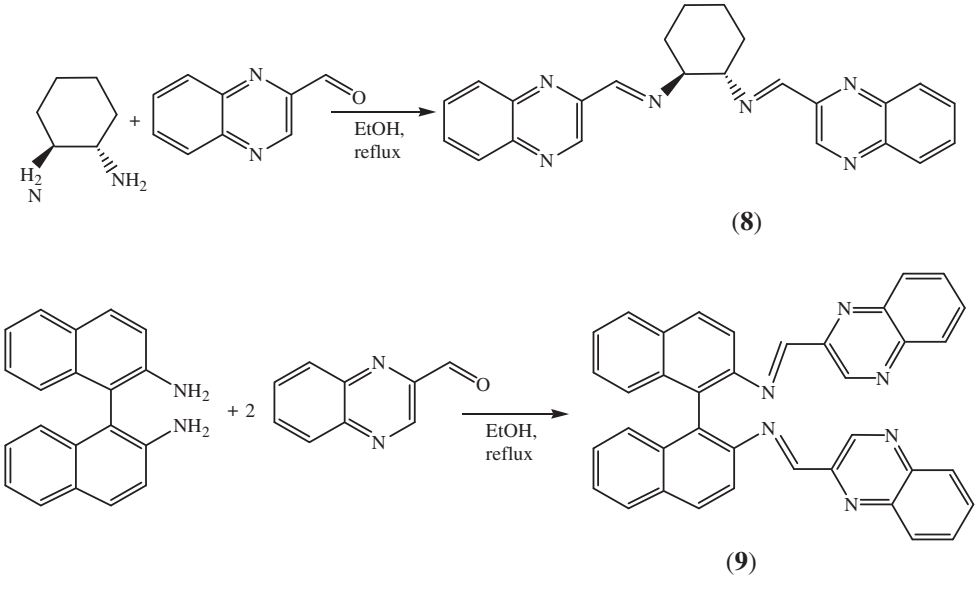

Scheme 3. Synthetic route of Schiff bases of quinoxaline-2-carboxaldehyde (**8** and **9**).

(**12**b) were synthesized and characterized by various spectral and analytical techniques. From the results, the following structures were assigned for the complexes (figure 6) [48].

New Co(III), Ni(II), and Cu(II) complexes of H-QTSC (**13**) (figure 7) have been prepared and characterized. The ligand is a uninegative tridentate NNS donor in the Co(II) and Cu(II) complexes and neutral bidentate NS donor in the Ni(II) complex. The cytotoxicity of Co(III) complex was determined *in vitro* as well as in tissue culture methods [49].

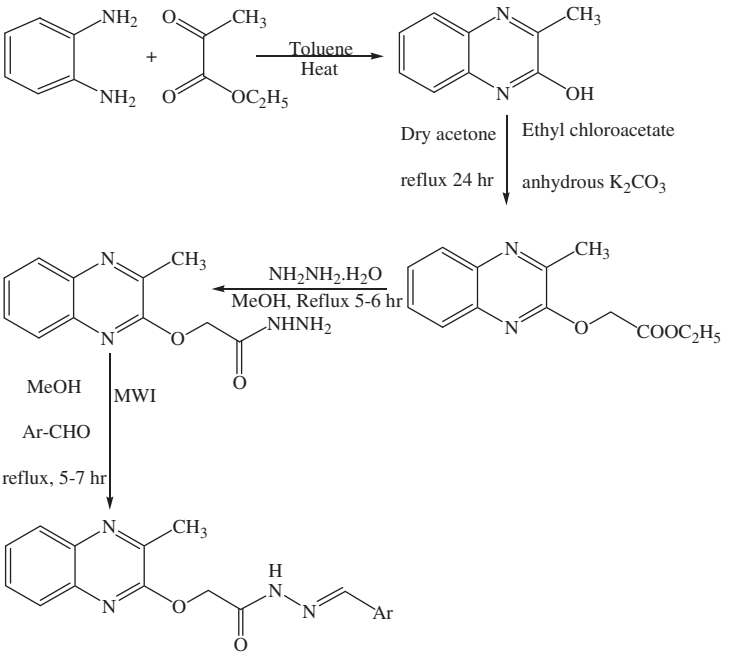

where Ar = Indole-3-carboxaldehyde (**10**a), Ar = Furfuraldehyde (**10**b), Ar = -(-4-nitrophenyl-2-furfuraldehyde (**10**c) and substituted benzaldehydes (Ar = C_6H_5, 4-ClC_6H_4, Ar = 3-$NO_2C_6H_4$, Ar = 4-OHC_6H_4, Ar = 3,4-$(OCH_3)C_6H_3$, Ar = 4-$(OCH_3)C_6H_4$, Ar = 4-$N(CH_3)_2C_6H_4$ (**10**d).

Scheme 4. Synthetic route of Schiff bases of 2-[(3-methylquinoxalin-2yl)oxy]acetohydrazide (**10**a–d).

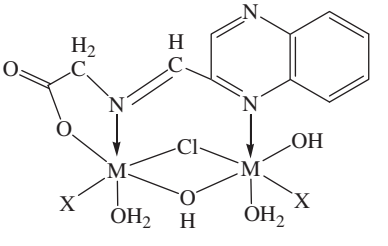

(M = Fe(III), Co(II), Ni(II) and Cu(II))

Figure 5. Structure of the complexes of QCG (**11**a).

Mn(II), Fe(III), Co(II), Ni(II), Cu(II), and Zn(II) complexes of a new dibasic multidentate ONNO donor H_2BSDHQ (**14**) were prepared and characterized [50]. Cr(III), Mn(II), Fe(III), Co(II), Ni(II), and Cu(II) complexes (**15**a–c and **16**a–d) of new tridentate oxygen–nitrogen donors, HSHQO (**15**) and HAHQO (**16**), were prepared and characterized. The analytical data indicate that M:L stoichiometry is 1 : 1 in Cr(III), Mn(II), and Fe(III) complexes of **15** and Cr(III) and Cu(II) complexes of **16**. The ratio is 1 : 2 in Co(II), Ni(II) and Cu(II) complexes of **15** and Fe(III), Co(II), Ni(II), and Cu(II) complexes of **16**. Cr(III) and Fe(III) complexes of **15** and **16** behaved as 1 : 1 electrolytes (figure 8) [51].

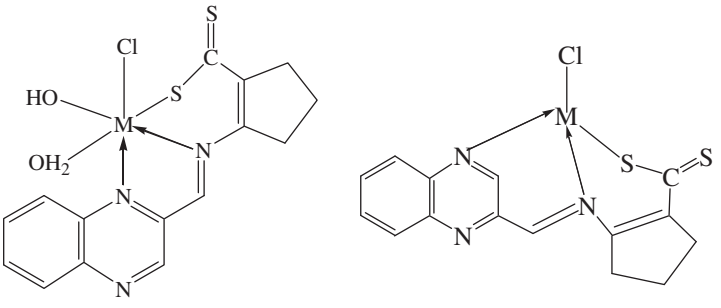

(**12**a) (**12**b)

Figure 6. Structure of metal complexes (**12**a and b).

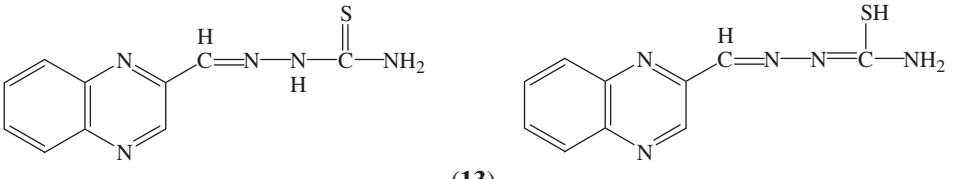

(**13**)

Figure 7. Structure of tautomeric structures of QTSC (**13**).

Synthesis, characterization, and catalytic activity studies of metal complexes of Schiff bases, N,N′-bis-(3-3hydroxyquinoxaline-2-carboxalidene)-ethylenediamine (**17**), N,N′-bis-(3-hydroxyquinoxaline-2-carboxilidene)-o-phenylenediamine-3-hydroxyquinoxalinehydrazone (**18**), and N,N′-bis-(3-hydroxyquinoxaline-2-carboxilidene)diethylenetriamine (**19**), were reported. The complexes of **17**–**19** exhibit anomalous magnetic behavior [52]. New complexes of Mn(II), Fe(III), Co(II), Ni(II), and Cu(II) with BHQ (**20**), QHA (**21**), QHS (**22**), QHF (**23**), and QHT (**24**) (figure 9) have been synthesized and characterized. The synthesized complexes have been screened for catalytic activity in oxidation of 3,5-ditert-butylcatechol to the corresponding quinone using molecular oxygen as the oxidant [53].

Some new transition metal complexes of the Schiff base QAP (**25**) were synthesized and characterized by elemental analysis, molar conductance, magnetic measurements, IR, and UV–Vis studies. The complexes of Mn(II), Co(II), Ni(II), and Cu(II) have empirical formula $[M(QAP)_2]$ and Fe(III) complex has the empirical formula $[Fe(QAP)_2Cl]$. The very low molar conductance values indicate non-electrolytes. A tetrahedral geometry was assigned for Mn(II), Co(II), Ni(II), and Cu(II) complexes (**25**a) except Fe(III) (**25**b), which has an octahedral geometry (figure 10) [54].

Two series of transition metal complexes of QSC (**26**) and QFA (**27**) were synthesized (figure 11) [55] and characterized by elemental analysis, molar conductance, magnetic susceptibility measurements, IR, electronic and electron paramagnetic resonance (EPR) spectral studies. The molar conductance values show that **26**a, **26**b, and **27**a are

non-electrolytes. All the complexes exhibit catalytic activity towards oxidation of 3,5-di-tert-butylalcohol to 3,5-di-tert-butylquinone, using atmospheric oxygen.

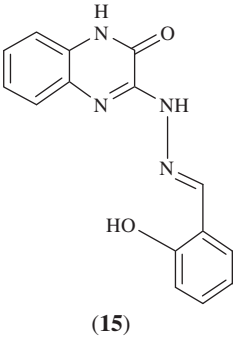

(**15**)

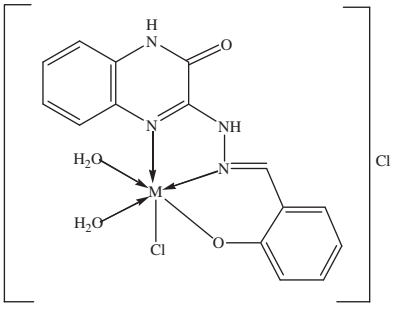

M = Cr(III) or Fe(III)

(**15**a)

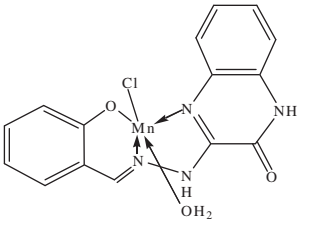

(**15**b)

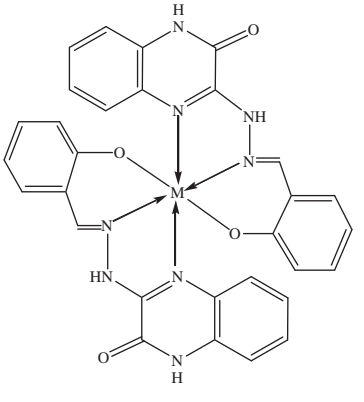

M= Co(II), Ni(II), Cu(II)

(**15**c)

Figure 8. Structures of HSHQO (**15**), HHAHQO (**16**) and their metal complexes (**15**a–c and **16**a–d).

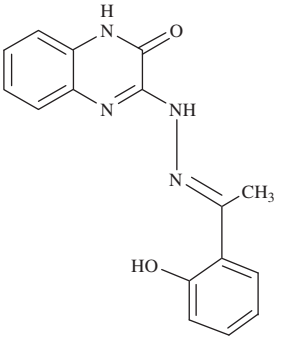

(**16**)

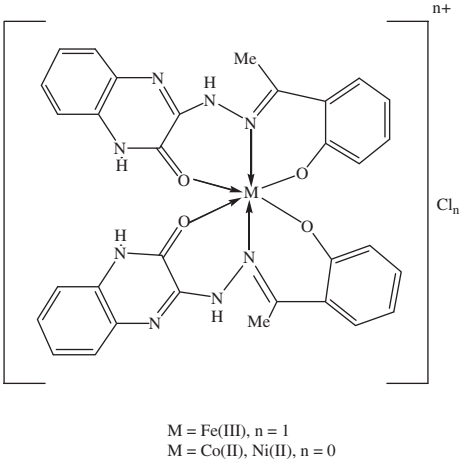

M = Fe(III), n = 1
M = Co(II), Ni(II), n = 0

(**16**a)

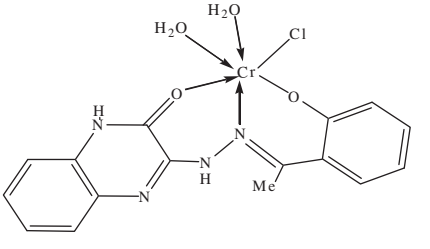

(**16**b)

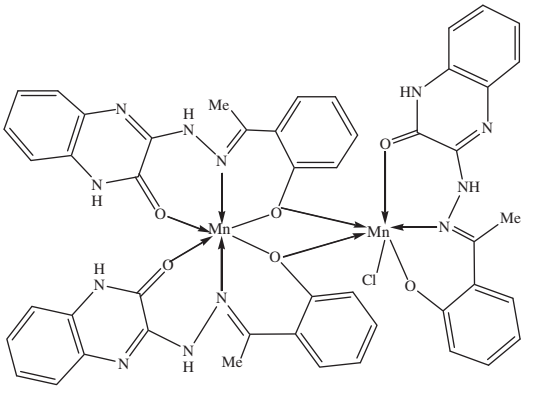

(**16**c)

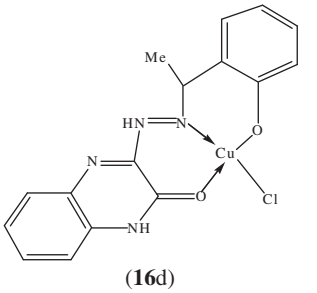

(**16**d)

Figure 8. *(Continued)*.

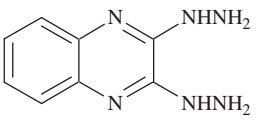

(**20**)

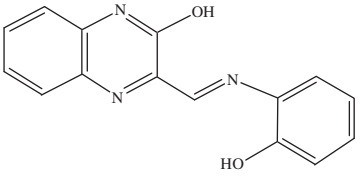

(**21**)

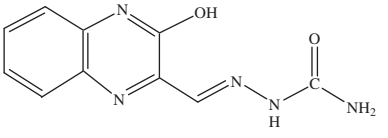

(**22**)

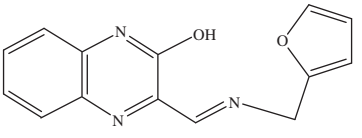

(**23**)

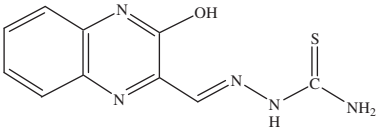

(**24**)

Figure 9. Structures of BHQ (**20**), QHA (**21**), QHS (**22**), QHF (**23**), and QHT (**24**).

Zeolite-encapsulated Co(II), Ni(II), and Cu(II) complexes of QED (**28**), QPD (**29**), QHD (**30**), and QDT (**31**) were synthesized and characterized (figure 12) [56].

The synthesis, characterization, and assignment of possible geometries of polymer-anchored Schiff base (PS-HQAD) (**32**) complexes of Co(II), Ni(II), and Cu(II) were reported (PS-HQAD was prepared by condensation of polymer-bound amine with 3-hydroxyquinoxaline-2-carboxaldehyde) (figure 13) [57].

Wang *et al.* [58, 59] reported the design and synthesis of a chemo selective sensor for mercury ion containing quinoxaline. Four new polymeric Ag(I) complexes based on 2,5-bis(2-benzodiazine)-3,4-diaza-2,4-hexadiene (**33**) with disubstituted quinoxalinediazenes were characterized by IR, elemental analysis, and single-crystal X-ray diffraction [60].

Gamo [61] reported the synthesis of Ni(II) and Cu(II) complexes with QXDO (**34**) and their characterization using physico-chemical techniques. Metal complexes of a new multidentate ligand with two different N-heterocyclic constituents were synthesized. BQXDP (**35**) and its Cd(II), Ni(II), Zn(II), Fe(II), Cr(III), Mn(II), and VO(IV) complexes were prepared and characterized by IR, ^{1}H and ^{13}C NMR, electronic spectra, and elemental analysis [62].

Che *et al.* [63] reported synthesis of 8-carboxyindenol[1,2-b]-quinoxaline-11-one thiosemicarbazone (**36**) Zn(II) complexes. Zn(II) is five-coordinate and situated in a distorted square-pyramidal environment. Ru(III) complexes of QAP (**25**), QPD (**29**), and QAB (**37**) were synthesized and characterized by elemental, spectral (IR, UV–Vis, EPR and FAB mass), thermogravimetric, molar conductance, and magnetic moment analysis. The synthesized new ligands and their complexes have been tested for *in vitro* growth-inhibitory

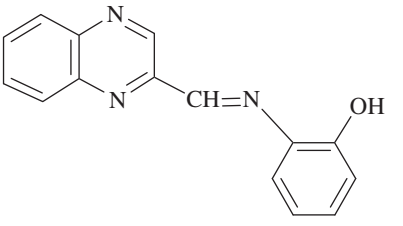

(**25**)

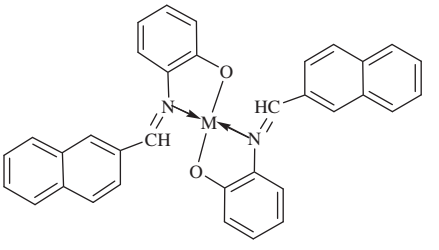

[M = Mn(II), Co(II), Ni(II) or Cu(II)]

(**25**a)

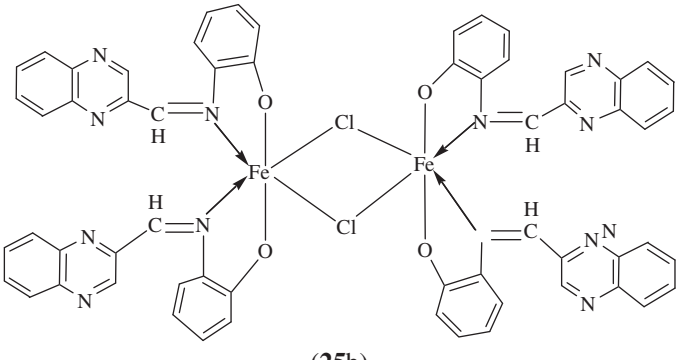

(**25**b)

Figure 10. Structures of QAP (**25**) and its complexes (**25**a and b).

activity against one strain of gram-positive bacteria *Klebsiella pneumoniae* and gram-negative bacteria *Escherichia coli* and *Pseudomonas aeruginosa*. The complexes are active while the ligands are inactive toward the bacteria under study (figure 14) [64].

Chittilapilly *et al.* [65] synthesized and characterized zeolite-Y-encapsulated Ru(III) complexes of **25**, **29,** and **37** (RuYqap, RuYqpd, and RuYqab, respectively). These complexes except, RuYqpd, catalyze catechol oxidation by H_2O_2 to 1,2,4-trihydroxy benzene. New Cr(III), Mn(II), Fe(III), Ni(II), and Cu(II) complexes of NBHQO (**38**) were synthesized and characterized by elemental analysis, molar conductance, thermal, spectral and magnetic data. Analytical data indicate that the metal-to-ligand stoichiometry is 1 : 2 except in Cu(II) complex where it is 1 : 1. Cr(III) and Fe(III) complexes are 1 : 1 electrolytes, Ni (II) complex is 1 : 2 electrolyte, and Mn(II), Co(II), and Cu(II) complexes are non-electrolytes. Compound **38** is a bidentate ON donor in all the complexes except the Ni(II)

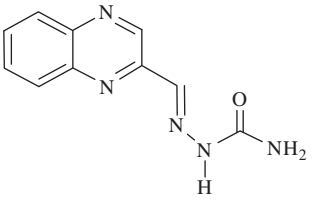

(**26**)

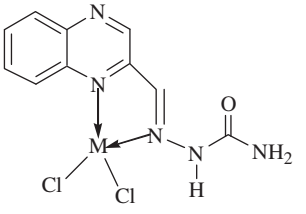

(M=Mn(II), Co(II) and Ni(II))

(**26**a)

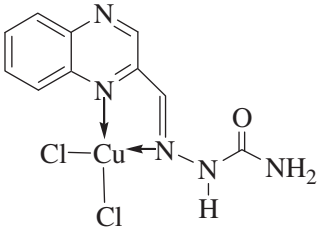

(**26**b)

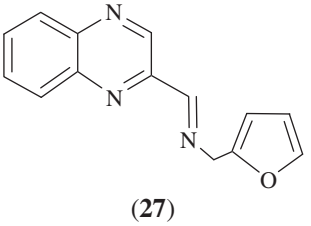

(**27**)

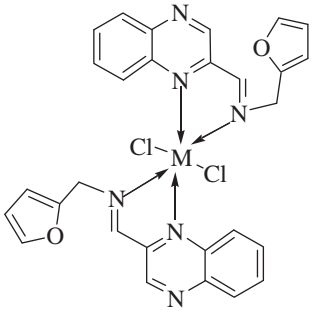

(M = Mn(II), Co(II), Ni(II) and Cu(II))

(**27**a)

Figure 11. Structure of QSC (**26**) and QFA (**27**) and their metal complexes (**26**a and b and **27**a).

complex, in which it is a tridentate ONO donor. Octahedral geometries have been proposed for all the complexes (**38**a and **38**b), except for Cu(II) (**38**c) which has square planar geometry (figure 15) [66]. Metal complexes of 2-quinoxalinolsalen (**39**) were synthesized, characterized and their applications were studied [67, 68].

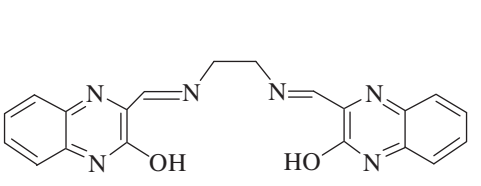

(**28**)

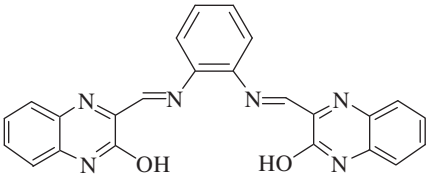

(**29**)

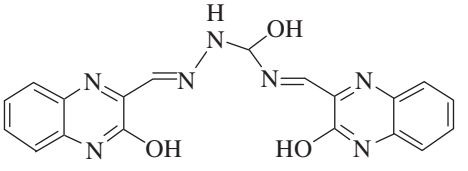

(**30**)

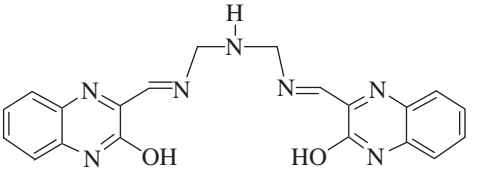

(**31**)

Figure 12. Structure of QED (**28**), QPD (**29**), QHD (**30**), and QDT (**31**).

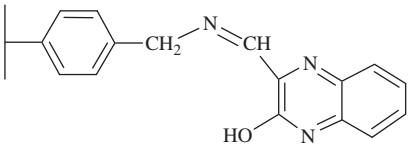

Figure 13. Structure of PS-HQAD (**32**).

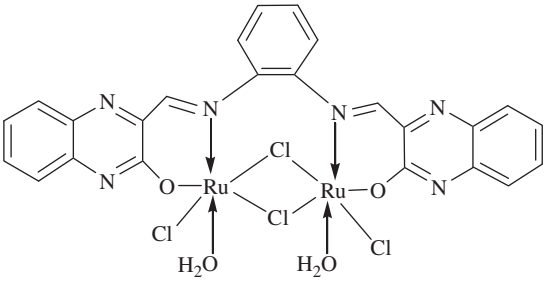

Figure 14. Structure for Ru(III) complex of QPD (**29**).

Metal complexes of heterocyclic multidentate ligands containing triazine and quinoxaline were synthesized by template method and characterized. The ligand was coordinated to metal as a dibasic tridentate (ONN) ligand. The studies reveal tetrahedral and octahedral geometries for the Zn(II) and Cu(II) complexes, respectively [69]. The VO(IV), Cu(II), and Ru(II) complexes of HQCDMN-H_2 (**5**), hqcdan-H_2 (**40**), HQCDAC-H_2 (**41**), HQCAP-H_2 (**42**), and HQCAAP-H_2 (**43**) were synthesized and their catalytic activities towards oxidation and hydrogenation reactions have been reported [70]. The ligands show two tautomeric forms, enol (**40**a, **41**a, **42**a, and **43**a) and keto (**40**b, **41**b, **42**b, and **43**b) forms (figure 16).

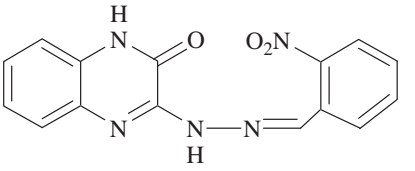

(**38**)

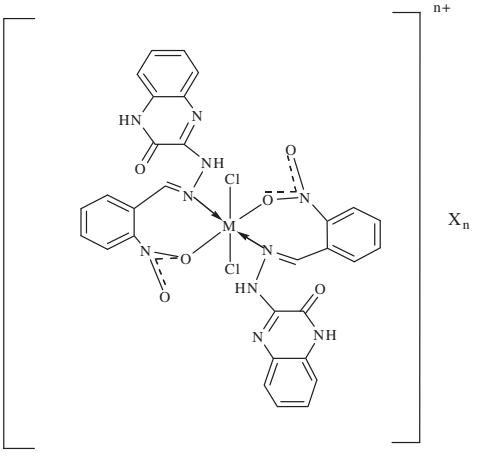

[M = Cr(III), Mn(II), Fe(III) or Co(II); X = Cl^-; n = 0 or 1]

(**38**a)

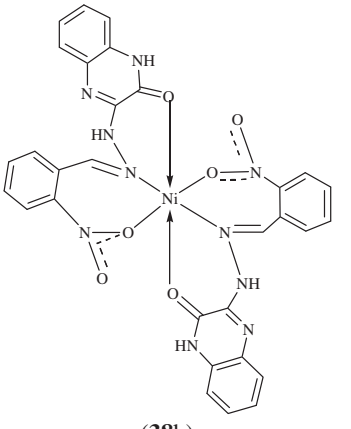

(**38**b)

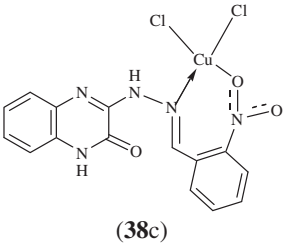

(**38**c)

Figure 15. Structure of NBHQO (**38**) and its metal complexes (**38**a–c).

A series of new Cr(III), Mn(II), Fe(III), Co(II), Ni(II), and Cu(II) complexes of Schiff base HDHAHQO (**44**) (figure 17) [71] were prepared from HQO and DHA and characterized. The Schiff base exhibits bi-ambidenticity, as monobasic tridentate ONN donor in Cr (III), Mn(II), Co(II), and Ni(II) complexes. Mononuclear Co(II) complex $[CoL_2]\cdot H_2O$ was prepared (where HL=quinoxaline-2-carboxalidene-2-amino-5-methylphenol) (**45**) and characterized [72]. The characterization techniques include elemental analysis, conductivity

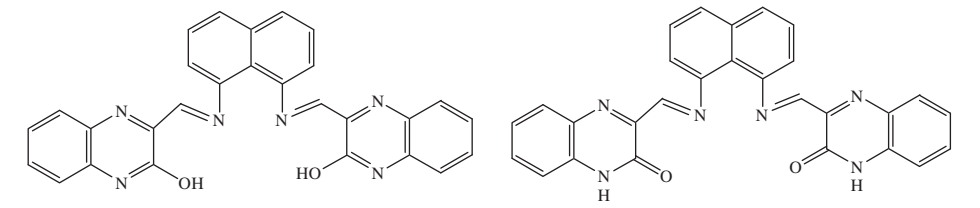

(**40**a) (**40**b)

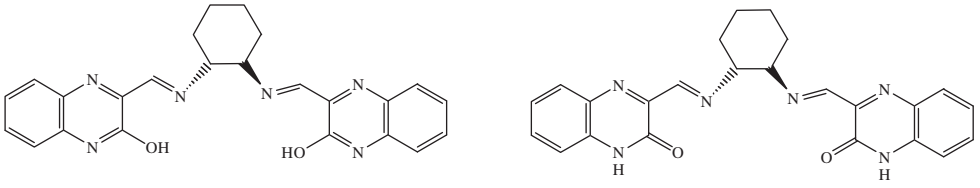

(**41**a) (**41**b)

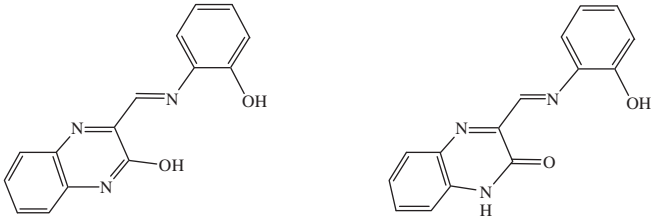

(**42**a) (**42**b)

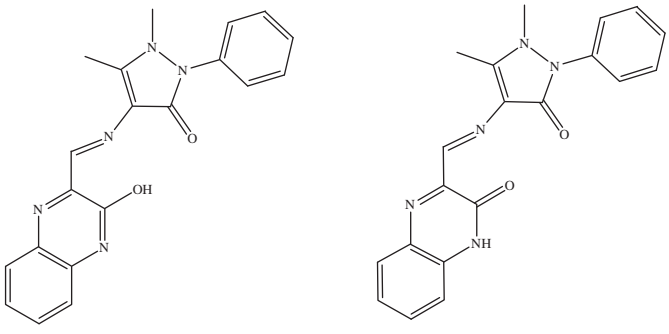

(**43**a) (**43**b)

Figure 16. Tautomeric structures of hqcdan-H_2 (**40**), HQCDAC-H_2 (**41**), HQCAP-H_2 (**42**), and HQCAAP-H_2 (**43**).

measurements, IR, UV–Vis, TG-DTA, and XRD. The crystallographic study shows that Co(II) is distorted octahedral with each tridentate NNO Schiff base *cis*. They also reported [73] the synthesis and characterization of Mn(II), Fe(III), Ni(II), Cu(II), and Zn(II) complexes of **45**. The structure of $[NiL_2]\cdot H_2O$ was studied by single-crystal XRD. All the prepared complexes were screened for their catalytic activity for liquid phase hydrogenation of phenol.

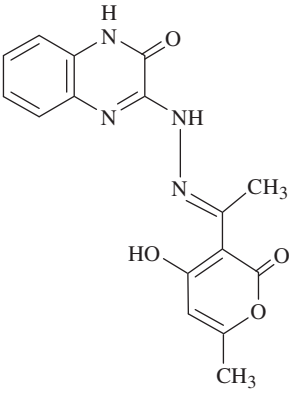

(**44**)

Figure 17. Structure of HDHAHQO (**44**).

Two new complexes of $[ML(H_2O)]\cdot H_2O$ (**43**c) (figure 18) {where M=Ni(II) or Ru(II) and L (**43**)} were synthesized and characterized by elemental analysis, IR, UV–Vis, diffuse reflectance spectroscopy, FAB-mass, TG-DTA, atomic absorption spectroscopy, cyclic voltammetry, molar conductance, and magnetic susceptibility measurements. The complexes have a distorted octahedral structure and are effective catalysts for hydrogenation of benzene [74, 75].

Budagumpi *et al.* [76] reported synthesis and characterization of a series of Co(II), Ni (II), Cu(II), and Zn(II) complexes of 1H-pyrazolo-3,5-dicarboxylic(2-hydroxy-3-hydrazinoquinoxaline) (**46**). DNA binding/cleavage studies revealed stronger binding of the Ni(II) complex, confirmed by absorbance, viscometric, and gel electrophoresis studies. Cu(II) complex shows growth-inhibitory activity.

Rai *et al.* [77] reported the synthesis, characterization, and antimicrobial screening of Co(II), Ni(II), and Cu(II) complexes with AQSC (**47**). **47** behaves as a neutral bidentate chelating agent, bonded through azomethine nitrogen and oxygen of semicarbazone. A new benzothiozoline derivative, BTQ (**48**), was synthesized (scheme 5) [78].

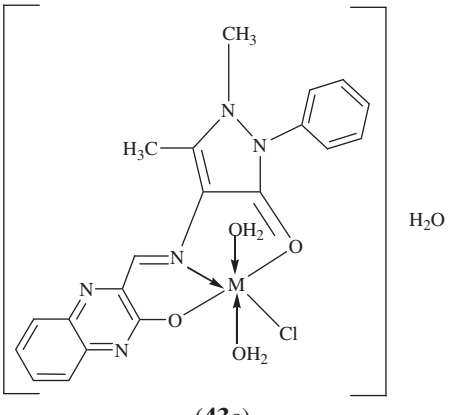

(**43**c)

Figure 18. Structure of metal complexes of HQCAAP-H_2 (**43**c).

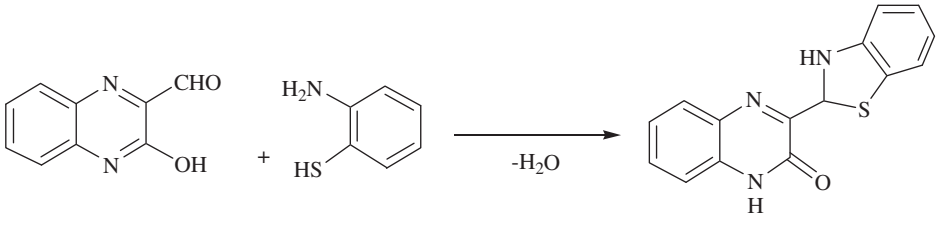

(**48**)

Scheme 5. Synthetic route of BTQ (**48**).

The Schiff base was prepared by condensation of 3-hydroxyquinoxaline-2-carboxaldehyde with 2-mercaptoaniline. They prepared complexes of Mn(II), Co(II), Ni(II), Cu(II), and Zn(II). All compounds have been characterized by elemental analysis, IR, electronic spectra, TG, molar conductance, and magnetic susceptibility measurements. Complex formation proceeds with rearrangement of benzothiozoline to form corresponding Schiff base chelates. The quinoxaline moiety of the ligand and its complexes exhibits keto–enol tautomerism (**48**a) (figure 19). All complexes show octahedral geometry, except Cu(II) and Zn(II), which have square planar and tetrahedral geometries, respectively.

Kurdekar *et al.* [79] reported a series of Co(II), Ni(II), Cu(II), and Zn(II) complexes of bi and tridentate hydrazones prepared by condensation of 2-mercapto-3-hydrazinoquinoxaline with 2-hydroxy-3-formylquinoline (L^1) (**49**) and 3-acetyl coumarin (L^2) (**50**), respectively (scheme 6). The compounds, characterized by various analytical techniques and magnetic moment studies, were monomeric and non-electrolytes. All complexes have octahedral geometry (**49**a), except Cu(II) (**49**b) which has square-pyramidal geometry, and all complexes of **50** have octahedral geometry (**50**a) (figure 20).

Kulkarni *et al.* [80] synthesized new binuclear transition metal complexes of bicompartmental SNONS-donor Schiff base obtained by condensation of 3-hydrazinyl quinoxaline-2 (1H)-thione with 2,6-diformyl-4-methyl phenol (**51**). The synthesized compounds were characterized by various physico-chemical techniques. Influences of two metal centers in terms of cooperative effect on electronic, magnetic, electrochemical, and structural properties were investigated.

The Schiff base compounds N,N′-((5,5′(quinoxaline-2,3-diyl)bis(1H-pyrrole-5,2-diyl))bis (methanylylidene)bis(4-methoxyaniline) (**52**) and N,N′-((5,5′(quinoxaline-2,3-diyl)bis(1H-pyrrole-5,2-diyl))bis(methanylylidene)dianiline) (**53**) have been prepared by Hu *et al.* [81].

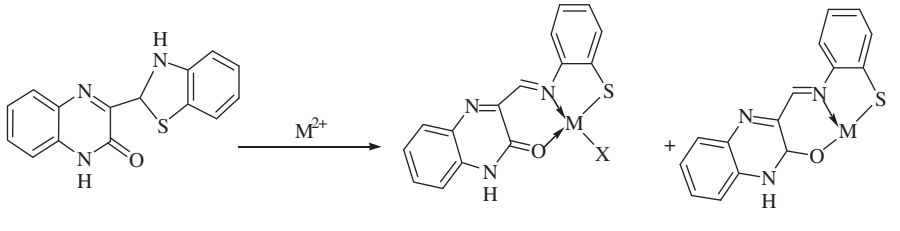

Keto form
M=Mn, Cu or Zn
(X = OAc for Mn and Zn, Cl for Cu)

Enol form
M = Co or Ni

Figure 19. Keto–enol tautomerism of btq (**48**a).

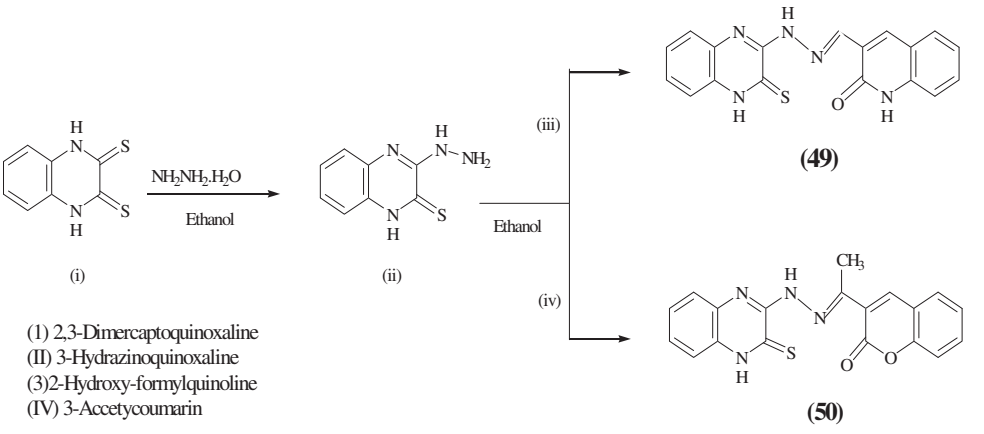

Scheme 6. Preparation of ligands (**49** and **50**).

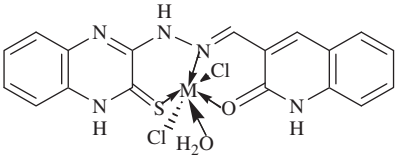

where M = Co(II), Ni(II) or Zn(II)

(**49**a)

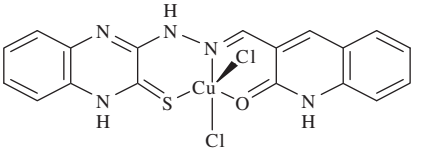

(**49**b)

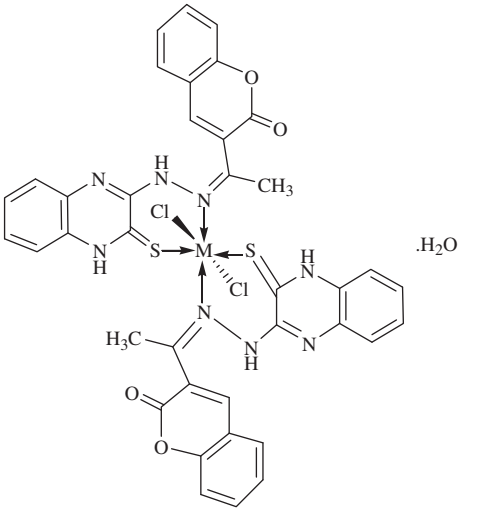

where M=Co, Ni, Cu and Zn

(**50**a)

Figure 20. Structure of metal complexes of **49** and **50**.

These compounds displayed good sensitivity toward transition-metal ions with Cd(II) and Zn(II) turn-on and Cu(II) and Hg(II) turn-off fluorescence. The fluorescence and crystal structure data indicate that 1 : 1 stoichiometry complex was formed with **52** or **53** and metal ions. Ligational behavior of Schiff bases prepared by condensation of 3-hydrazinyl-quinoxaline-2(1H)-thione with isatin (L^1) (**54**) and quinoxaline-2,3(1,4H)-dione (L^2) (**55**) and their metal complexes with first-row transition metal ions have been reported by Kulkarni *et al.* [82]. The compounds were characterized by spectro-analytical techniques and magnetic susceptibility measurements. All complexes show octahedral geometry and are mononuclear.

Kumar *et al.* [83] synthesized complexes $[M(AQTC)_2X_2]$ (where M=Co(II), Ni(II) or Cu(II), X=Cl^-, Br^-, I^-, and NO_3^-). The analytical and spectral data proposed that AQTC (**56**) is a neutral bidentate ligand bonded to metal through azomethine nitrogen and sulfur from the thiosemicarbazone. The remaining coordinating positions are satisfied by Cl^-, Br^-, I^-, and NO_3^-. Electronic spectra and magnetic susceptibility values revealed octahedral geometry for the complexes. The molar conductance indicates non-electrolytes. The ligand and its metal complexes have been screened for antibacterial and antifungal activity.

The synthesis and spectral characterization of Schiff base complexes obtained by template method (QLH) (**57**) were reported (scheme 7) [84]. The physico-chemical and spectrochemical measurements revealed square planar geometry for Cu(II) (**57**d) complex, tetrahedral geometry for Mn(II) and Zn(II) (**59**c) complexes, and octahedral geometry for Fe(III) (**57**b) and Ni(II) (**57**a) complexes (figure 21).

New transition metal complexes of quinoxaline–thiosemicarbazone ligands were prepared and characterized by spectro-analytical techniques. The ligands were obtained by condensation of quinoxaline-2,3(1,4H)-dione with methyl (**58**) and phenylthiosemicarbazide (**59**) (scheme 8). Some of the synthesized compounds exhibit antidiabetic activity [85].

The Schiff base prepared by condensation of 4-isopropylbenzaldehyde and 2-hydroxy-3-hydrazinoquinoxaline (**60**) has been synthesized and characterized [86]. A series of Ni(II) complexes have been prepared using **60**. Novel 2,3-bis(1H-pyrrol-2-yl)quinoxaline-functionalized hydrazones were prepared and characterized as new chemosensors for Cu(II) by Guo *et al*. [87].

VO(IV) complexes of **15**, **16**, **38,** and **44** were reported [88]. The compounds were characterized on the basis of analytical, molar conductance, magnetic moment, IR, NMR, ESR, and electronic spectral data. **15** and **44** are monobasic tridentate ONN donors through phenolic oxygen and azomethine nitrogens, **16** is a monobasic bidentate ON donor through phenolic oxygen, azomethine (free) nitrogen, and **38** is a neutral bidentate ON donor through oxygen of nitro and azomethine (free) nitrogen.

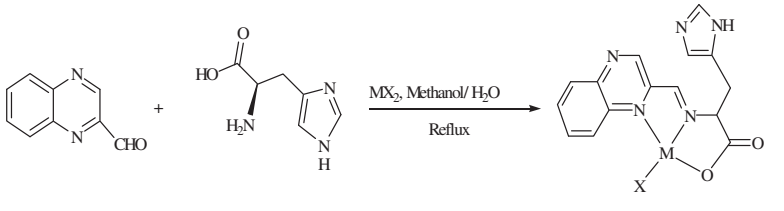

where M = Mn(II), Fe(III), Co(II), Ni(II), Cu(II) and Zn(II), X = CH_3COO^- for Mn(II), Co(II), Ni(II) and Zn(II), Cl^- for Fe(III) and Cu(II).

Scheme 7. Formation of complexes of QLH (**57**).

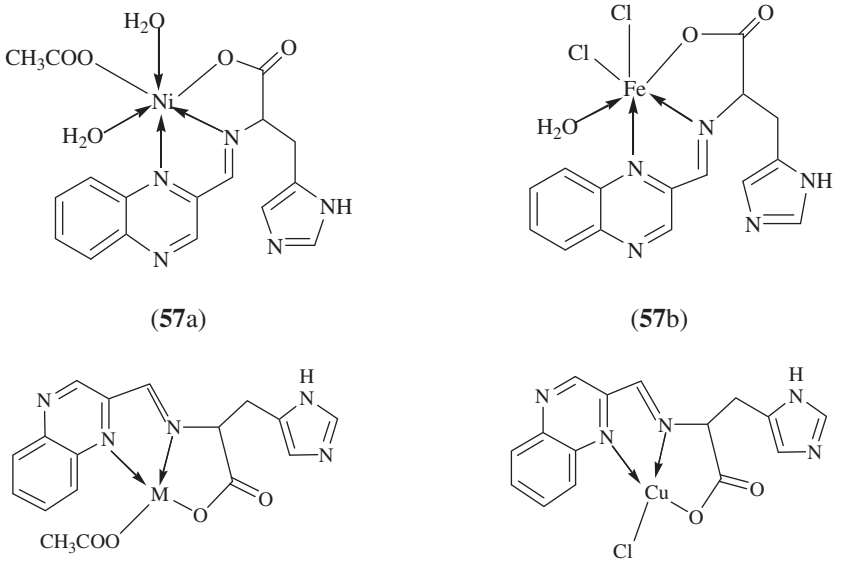

Figure 21. Structures of the complexes of QLH (**57**) (solvated water molecules are omitted).

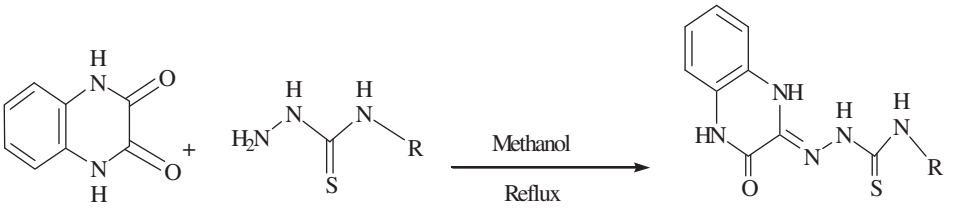

Scheme 8. Preparation of ligands (**58** and **59**).

5.1. *IR spectroscopy*

IR spectroscopy provides information as to whether reaction has occurred or not. The disappearance of certain absorptions and the appearance of new bands suggest that the product has been formed. IR spectral data of Schiff bases and their corresponding metal complexes give clear ideas about coordination sites in the ligands and mode of coordination towards the metal. On coordination, generally azomethine band shifts to lower wavenumber. IR data also give information about the presence of lattice water, coordinated water, hydrogen bonding, keto–enol tautomerism, and thio-amidic tautomerism. The presence of M–Cl terminal and bridging can also be determined from IR spectral data. The formation of new bands and disappearance of bands in spectra of metal complexes suggest formation of ν(M–O), ν(M–N) and ν(M–S) bonds.

Yusuff and Sreekala [46, 47] reported IR spectra of **11** and its Fe(III), Co(II), Ni(II), and Cu(II) complexes. A double hump around 3010 cm^{-1} was seen in the spectra of the complexes due to coordinated waters. New bands in all the complexes at 980 and 1180 cm^{-1} might be due to bridging OH bending and M–O–H bending, respectively. A band at 490 cm^{-1} due to υ(M–N) and another band at 460 cm^{-1} due to υ(M–O) are also observed in all the complexes.

Karthikeyan [48] reported IR spectra of **12** and its metal complexes. The Fe(III) complex shows bands at 3400 and 3060 cm^{-1} due to coordinated water and a band at 1605 cm^{-1} due to H-O–H deformation. A band at 500 cm^{-1} was assigned to υ(M–O) of coordinated water. A band at 1680 cm^{-1} in the spectrum of **12** may be attributed to υ(C=N). This band shifts to lower frequency around 1620 cm^{-1} in spectra of the complexes, indicating donation of the nitrogen electrons of azomethine to metal. The C=N (ring) stretch is a medium band at 1580 cm^{-1} in the ligand. In the complexes, this band lowers to 1570 cm^{-1} showing that nitrogen of the quinoxaline ring is coordinated. The 1000–900 cm^{-1} region is associated with C–S stretching frequencies in dithiocarboxylic acid complexes. In spectra of the complexes, there are more than three bands in this region, perhaps due to monodentate bonding of the dithiocarboxylic acid. The band at 965 cm^{-1} in the ligand is split in the complexes at 950 and 980 cm^{-1} and may be attributed to υ(C–S) and υ(C=S), respectively. Thus, **12** in these complexes is a tridentate ligand coordinated through nitrogen of azomethine, nitrogen of quinoxaline ring, and sulfur of the dithiocarboxylic acid. A strong band at 390 cm^{-1} in all complexes can be attributed to υ(M–S). The band at 450 cm^{-1} due to υ(M–N) and another band at 260 cm^{-1} due to υ(M–Cl) are also observed in all the complexes. In the Fe (III) complex, υ(M–O) is also observed at 500 cm^{-1}.

IR spectral data show that **13** is a uninegative tridentate or neutral bidentate ligand, depending on the metal salt used and the medium of the reaction. The ligand exhibits bands at 1640 and 1010 cm^{-1} due to υ(C=N) of azomethine and υ(N–N′), respectively. In spectra of all the complexes, υ(C=N) is at 1625 cm^{-1}, this red shift clearly suggesting involvement of azomethine nitrogen in bonding to metal. In the spectrum of the free ligand, υ(C=S) is a medium band at 780 cm^{-1}; on complexation, this band shifts to 730–700 cm^{-1} indicating participation of the sulfur in coordination [49].

IR spectra of **15** and **16** and their complexes have been reported by Lakshmi *et al.* [51]. IR spectra of **15** indicate binding of the metal through ONN involving phenolic oxygen and azomethine nitrogens. The absence of band at 3050 cm^{-1} in Co(II), Ni(II), and Cu(II) complexes suggests cleavage of intramolecularly hydrogen-bonded −OH with deprotonation and coordination through phenolic oxygen. The multi-structured broad band at 3600–2600 cm^{-1} in Cr(III), Mn(II), and Fe(III) complexes was attributed to υ(NH), υ(C–H), and υ(OH) (of coordinated water) and the appearance of band at 960–950 cm^{-1} confirmed the presence of coordinated water. New bands in the far IR were attributed to υ(M–O) and υ(M–N) in all complexes and 330–300 cm^{-1} attributed to υ(M–Cl) in Cr(III), Mn(II), and Fe(III) complexes. In IR spectra of complexes of **16**, υ(NH) in all complexes except Cr (III) was shifted to higher frequency. Disappearance of the υ(OH) band in the complexes indicates deprotonation of phenol. The band at 3400–2800 cm^{-1} for Cr(III) complex was assigned as υ(OH) (of coordinated water). Phenoxide binding in all the complexes was confirmed by shift of υ(CO). Negative shifts observed in υ(C=O) and υ(C=N) (exo) and upward shift of υ(N–N) indicate binding through carboxyl oxygen and one of the azomethine nitrogens. The υ(M–Cl) was identified at 330 cm^{-1} in Cr(III) and Cu(II) complexes.

IR spectra of **26**, **27** and their complexes were assigned [55]. **26** is a bidentate ligand, coordinating through the azomethine and ring nitrogens. The ligand exhibits a band at

1710 cm^{-1} due to combination of υ(C=N) of the azomethine and υ(C=O) of the semicarbazone. **26** exhibits a strong band at 1585 cm^{-1} assigned for υ(C=N) of the quinoxaline ring, shifted to 1545 cm^{-1}, indicating coordination of ring nitrogen to metal in all cases. **27** exhibits a strong band at 1675 cm^{-1} corresponding to υ(C=N) of azomethine, which is shifted to 1640 cm^{-1} in all complexes, indicating coordination of azomethine. The υ(C=N) for quinoxaline ring at 1584 cm^{-1} in the ligand undergoes a red shift to 1560 cm^{-1} in spectra of the complexes, indicating that the ring nitrogen was also coordinated to metal. IR spectral studies suggest that **27** is bidentate in all the complexes.

Suja and Yusuff [57] reported IR spectra of **32** and its complexes. Compound **32** gives azomethine band at 1660 cm^{-1}, red shifted on complexation, indicating coordination of azomethine. The C–N stretch of aromatic nitrogen at 1460 cm^{-1} shifts to lower frequencies due to shift in electron density from oxygen and nitrogen to metal.

IR spectra of **25**, **29,** and **37** showed a strong band at 1660–1630 cm^{-1} (characteristic for azomethine) in all the synthesized complexes. This band slightly shifted to lower frequency, indicating coordination of Schiff base through azomethine. IR spectral bands at 860–810 cm^{-1} indicate the presence of coordinated water and spectral band at 370 cm^{-1} indicates the presence of terminal chloride [64]. Bands at 310 and 145 cm^{-1} indicate the presence of bridged chloride in the complexes.

Chittilapilly *et al.* [65] reported IR spectra of some zeolite-encapsulated complexes of **25**, **29,** and **37**. The IR band at 1640 cm^{-1} in the ligand shifted to lower frequencies in all zeolite-encapsulated complexes, confirming complexation at nitrogen of azomethine. Sharp bands at 1300–1270 cm^{-1} in free ligands are masked by the zeolite broad band at 1000 cm^{-1} in all the encapsulated complexes. A sharp band in all encapsulated complexes at 1030–1020 cm^{-1} is due to the zeolite framework vibration; it is not present in the corresponding free ligands. IR spectra of all zeolite-encapsulated complexes show bands at 1570–1500 cm^{-1}, assigned for C–C stretch of benzene.

The IR spectrum of **38** shows bands at 1540 and 1520 cm^{-1} for free υ(C=N) and ring υ(C=N), respectively. On complexation, υ(C=N) (free) in all the complexes undergoes a downward shift by about 20 cm^{-1}, merging with the ring υ(C=N). This shows that free azomethine nitrogen participated in M–L bonding. In all the complexes, an upward shift of $\upsilon_{sym}(NO_2)$ by 20 cm^{-1} and a downward shift of $\upsilon_{asym}(NO_2)$ by 10–20 cm^{-1} indicate binding of NO_2 through oxygen. The absence of a sharp peak at 600 cm^{-1} (corresponding to the NO_2 wagging mode of ligand) further confirms coordination of one oxygen of NO_2. In Ni(II) complex, the downward shift of υ(C=O) confirms participation of carbonyl oxygen coordination [66].

Arun *et al.* [74] reported IR spectra of **43** and its Ni(II) and Ru(II) complexes. The strong υ(C=O) at 1670 cm^{-1} is due to amide–iminol tautomerism. The phenolic stretch observed at 1306 cm^{-1} in the free Schiff base shifted to 1312 and 1310 cm^{-1} in spectra of the Ru(II) and Ni(II) complexes, respectively, giving evidence for coordination through the enolate oxygen in the iminol form. The band at 1656 cm^{-1} due to υ(C=O) of the antipyrine part of the ligand shifting to 1650 cm^{-1} in the complexes indicates involvement of C=O in coordination.

The IR spectral data of **45** have been reported [72]; υ(C=N) of azomethine and quinoxaline ring appear as a group of bands at 1630–1520 cm^{-1}. Weak bands at 3060–2800 cm^{-1} are assigned for C–H stretch. Peaks at 3500–3300 cm^{-1} for the complexes are due to (O–H) stretching vibrations of lattice water and indicate hydrogen bonding. The band at 935 cm^{-1} for the complex is attributed to bending vibrations of water. The complex displays a medium peak at 1667 cm^{-1} due to azomethine υ(C=N) shifted by 41 cm^{-1} to

higher energy compared to free ligand. This increase in azomethine stretching frequency on coordination might be due to extensive delocalization of π-electrons in fully conjugated Schiff base. The υ(C–O) (phenolic) stretch is observed at 1251 cm^{-1} in the complex.

Sebastian *et al.* [73] reported IR spectra of Mn(II), Fe(II), Ni(II), Cu(II), and Zn(II) complexes of **45**. The υ(C=N) at 1626 cm^{-1} of the Schiff base shifted to lower frequencies in metal complexes due to the coordination of azomethine. The C=N stretch of quinoxaline ring also undergoes a small shift (-5 cm^{-1}) on complexation indicating that ring nitrogens are also involved in coordination. The shift of υ(C–O) in all complexes to lower frequencies indicates participation of phenolic oxygen on chelation. The chloro complexes ([$FeLCl_2$ and [CuLCl]) show additional IR bands at 364 and 332 cm^{-1} which can be assigned to υ(M–Cl). The acetato complex, [MnL(OAc)], displays $\upsilon_{asym}(COO^-)$ and $\upsilon_{sym}(COO^-)$ at 1577 and 1390 cm^{-1}, respectively, consistent with monodentate acetate.

Sebastian *et al.* [78] reported IR spectral data for transition metal complexes of an ONS-donor Schiff base (**48**). The formation of benzothiozoline was confirmed due to the absence of υ(SH) in the spectrum of btq. The ligand shows two absorptions at 3375 and 3325 cm^{-1}, assigned for υ(NH) in the amide tautomer and benzothiozoline rings, respectively. The complexes exhibit a broad band at 3500–3100 cm^{-1} due to stretch of water. The (N–H) stretch was also observed in this region.

In the IR spectral study of **49**, **50** and their metal complexes [79], **49** and **50**, show sharp bands at 1608 and 1596 cm^{-1}, respectively, assigned to υ(C=N). These bands shift to lower frequency due to coordination of azomethine nitrogen. Bands at 1660 and 1725 cm^{-1} are attributed to υ(C=O) of quinoline and coumarin, respectively. The absence of band at 2500 cm^{-1} indicates stable thione form of the ligand. Coordination of the quinoline carbonyl is evidenced by negative shift for υ(C=O) in complexes. No shift in υ(C=O) in complexes evidences no coordination of (C=O) of coumarin in **50**. In all complexes of **49** and **50**, υ(C=S) shifted to lower frequencies indicating coordination of sulfur in thione. IR spectra also indicate the presence of coordinated or lattice water molecules. IR spectral studies of ligands and their complexes [80] indicate that the ligand acts as a bicompartmental SNONS donor. The coordination sites are phenolic −OH, thioamide and azomethine nitrogen. The phenolic groups were coordinated through deprotonation.

IR spectra of **54** and **55** were reported [82]. In both, the amine υ(NH) were observed as broad bands around 3180 cm^{-1} with a small shift and line broadening upon complexation. In **54**, an intense band at 1704 cm^{-1} was ascribed to lactonic carbonyl of isatin. Due to coordination of oxygen in the complexes, a reduction in intensity and shift in υ(C=O) were observed. For **55**, υ(C=O) was observed at 1681 cm^{-1} and experiences a negative shift upon complexation. The υ(C=N) observed at 1675 cm^{-1} in L^1 shifted to a lower frequency by -10–20 cm^{-1} upon complexation due to coordination of azomethine nitrogen. In both ligands, ring (C=N) stretches were observed around 1600 cm^{-1} and remained almost unaltered upon complexation. Thioamide bands having a major contribution from υ(C=S) were at 1293 and 767 cm^{-1} as sharp bands, undergoing considerable reduction in intensity and shifting to lower frequency upon complexation, suggesting coordination of the thione sulfur. The low-frequency non-ligand bands at 470 and 420 cm^{-1} were assigned to υ(M–N) and υ(M–S), respectively.

Kumar *et al.* [83] reported IR spectra of **56** and its metal complexes. A broad band of medium intensity at 1460 cm^{-1} was assigned as azomethine; in spectra of the complexes, this band shows red shift with slightly reduced intensity suggesting coordination of azomethine nitrogen. The IR band at 800 cm^{-1} was assigned for υ(C=S) with red shift in

complexes, indicating coordination through thione sulfur of thiosemicarbazone. From the IR spectral data, **56** is a neutral N, S donor.

IR spectral characterization of **57** and its complexes was reported [84]. The υ(C=O) in quinoxaline-2-carboxaldehyde at 1680 cm^{-1} is absent in spectra of complexes, confirming formation of Schiff base. Bands at 1660–1610 cm^{-1} attribute to asymmetric υ(COO^-) and υ(C=N) of azomethine. Spectra of acetato complexes have υ(COO^-) as a sharp band at 1650 cm^{-1}, masking υ(COO^-) of Schiff base. The symmetric υ(COO^-) is observed at 1420–1400 cm^{-1}. In spectra of all complexes, separation between $\upsilon_{asym}(COO^-)$ and $\upsilon_{sym}(COO^-)$ is 240–230 cm^{-1}, indicating monodentate acetate. The broad band at 3300 cm^{-1} in all the complexes indicates the presence of water, with coordinated water in Fe(III) and Ni(II) complexes confirmed by the sharp bending vibration at 800–750 cm^{-1}. The υ(N–H) of imidazole also occurs in this region. Bands at 1590–1550 cm^{-1} are assigned for (C=N) stretch of quinoxaline ring. The Schiff base exists in enol form in Co (II) and Ni(II) complexes, evidenced by the disappearance of (C=O) stretch, but it exists in the keto form in Mn(II), Cu(II), and Zn(II) complexes as there is a strong band at 1650, 1676, and 1657 cm^{-1}, respectively. All the complexes exhibit azomethine stretch at 1640 cm^{-1} and υ(CO) phenol stretch at 1300–1200 cm^{-1}. The appearance of new bands at 500–400 cm^{-1} in complexes are assigned for υ(M–O) and υ(M–N) vibrations.

Kulkarni *et al.* [85] reported IR spectral studies of Co(II), Ni(II), Cu(II), and Zn(II) complexes of **58** and **59** (scheme 8). The absence of a band at 2600–2500 cm^{-1} (characteristic of υ(CSH)) suggests the stable thione form of ligands. The thio-amidic-coupled vibrations at 1600, 1545, 1460, and 940 cm^{-1} confirm the thio–keto form of ligands. The υ(C=O) of quinoxaline ring was observed as a sharp intense band at 1675 cm^{-1} and υ(C=N) for azomethine at 1645 cm^{-1}. The quinoxaline ring υ(NH) and hydrazine υ(NH) were observed at 3300 cm^{-1} as broad intense bands. In all the complexes, the band due to υ(C=O) is not observed due to coordination of oxygen through enol mode. This is also confirmed by a new band for υ(C–O) at 1260 cm^{-1}. The band due to υ(C=N) has been shifted to lower frequency in all the complexes due to coordination of azomethine nitrogen. The υ(C=S) disappeared or decreased in intensity upon complexation, suggesting thioenolization and coordination of sulfur, further supported by the strong band at 760 cm^{-1} for υ(C–S). The absence of υ(S–H) in the complexes suggests coordination of sulfur through deprotonation.

5.2. *UV–visible spectroscopy*

Electronic absorption spectroscopy of transition metal complexes is widely used to study stereochemistry. The d-d transitions of the metal ions and their corresponding absorption spectra have been effectively used to determine the ligand-field splitting of the d-orbitals of the metal ions and hence their geometry in the resultant complexes. From electronic spectra of the free ligand and their complexes, we can get knowledge about the metal-–ligand interaction in the complexes.

Mayadevi *et al.* [54] reported the electronic spectra of complexes synthesized from **25**. In spectra of all complexes, a solvent-sensitive band at 333 nm was obtained, red shifted in more polar solvents. This broad band can be assigned to ligand-to-metal charge transfer transition. Absorptions at 250 and 213 nm were assigned to electronic transitions within the ligand. Electronic transitions from the $^6A_1$ ground term of Mn(II) to higher energy terms are spin-forbidden. However, the band appearing at 547 nm in the electronic spectrum of Mn(II) complex is assigned to $^6A_1 \rightarrow {}^4T_1(G)$ and is consistent with tetrahedral geometry. For the Co(II) complex, the band at 537 nm is assigned to the $^4A_2 \rightarrow {}^4T_1(P)$,

which is typical for tetrahedral Co(II) complexes. The band at 584 nm in the Ni(II) complex is assigned to the forbidden transition $^3T_1(F) \rightarrow {}^3T_1(P)$ due to the tetrahedral structure around Ni(II). Due to the distorted tetrahedral configuration, the Cu(II) complex shows a broad band at 602 nm for $^2T_2 \rightarrow {}^2E$ transition. The low energy bands around 2000 nm in Co(II) and Ni(II) complexes are due to $^4A_2 \rightarrow {}^4T_1(F)$ and $^3T_1 \rightarrow {}^3A_2(F)$ transitions, respectively.

Electronic spectra of complexes of **26** and **27** in methanol and in solid state were reported [55]. In the Mn(II) complex, transitions not observed due to the electronic transitions from $^6A_1$ ground state of Mn(II) to higher states are spin-forbidden. The electronic spectrum of Co(II) complex of **26** shows absorptions at 536 nm, assigned for the transition $^4A_2 \rightarrow {}^4T_1(P)$ and a low energy band at 1437 nm attributed to $^4A_2 \rightarrow {}^4T_1(F)$ also supports tetrahedral configuration. From the bands obtained, tetrahedral geometry is assigned for the Co(II) and Ni(II) complexes and a tetragonal configuration is assigned for the Cu(II) complex. Spectra of all the complexes of **26** exhibit strong bands due to n–π^* transitions around 312 and 357 nm assigned to charge transfer transition. The Mn(II) complex of **27** shows a weak band at 461 nm due to $^6A_{1g} \rightarrow {}^4T_{2g}(G)$ transition of octahedral Mn(II). In the Co(II) complex, the d-d transitions are almost masked by the high-intensity charge transfer bands, but a shoulder is observed around 454 nm assigned for $^4T_{1g}(F) \rightarrow {}^4T_{1g}(P)$ transition of octahedral Co(II) complexes. The Ni(II) complex of QFA shows a strong band corresponding to octahedral geometry at 568 nm. The Cu(II) complex exhibited a broad d-d band at 847 nm assigned for octahedral geometry of Cu(II) complex. In all complexes of **27**, a strong band at 250 nm was assigned for the n–π^* transition and charge transfer transitions at 370–303 nm.

The electronic spectral data of some encapsulated Ru(III) complexes of **25**, **29,** and **37** were reported [65]. Normally in encapsulated Ru(III) complexes, the charge transfer absorption occurs at relatively low energies. Here, the electronic spectra of encapsulated Ru(III) complexes exhibit high intensity bands above 333 nm assigned as charge transfer bands. RuYqpd shows absorption as shoulder on the intense charge-transfer band at 351 nm assigned to the transition $^2T_{2g} \rightarrow {}^2A_{2g}$, $^2T_{1g}$. Bands at 568–588 nm have been assigned to spin-forbidden transitions.

The electronic spectra of metal complexes derived from **38** were reported [66]. Spectral studies suggest octahedral geometry except for Cu(II) complex, which has square planar geometry. The inter-electronic repulsion (B) and nephelauxetic parameter (β) were evaluated for the Ni(II) complex, which indicate a moderate field strength due to the tridentate ligand.

Arun *et al.* [74] reported solution state and solid phase electronic spectra of Ni(II) and Ru(II) complexes of **43**. The diffused reflectance spectrum of Ru(II) shows Ru(II) in an octahedral environment. Four bands corresponding to the transitions $^1A_{1g} \rightarrow {}^3T_{1g}$, $^1A_{1g} \rightarrow {}^3T_{2g}$, $^1A_{1g} \rightarrow {}^1T_{1g}$, and $^1A_{1g} \rightarrow {}^1T_{2g}$ are possible in increasing energy. The shoulders at 645, 840, and 1422 nm might be due to $^1A_{1g} \rightarrow {}^1T_{1g}$ and spin-forbidden $^1A_{1g} \rightarrow {}^3T_{2g}$, and $^1A_{1g} \rightarrow {}^3T_{1g}$ transitions, respectively. Octahedral or pseudo-octahedral Ni (II) complexes have three-spin-allowed d-d transitions. In the visible region of the spectrum, one band corresponding to $^3A_{2g}(F) \rightarrow {}^3T_{1g}(P)$ transition is at 480 nm. The bands at 1672 nm may be due to the spin-forbidden $^3A_{2g}(F) \rightarrow {}^1E_g(D)$ transition.

The band at 385 nm of **45** shifted to 370 nm on complexation indicating coordination of azomethine nitrogen with Co(II). The band at 539 nm is due to the $^4T_{1g}(F) \rightarrow {}^4A_{2g}(F)$. The intensity of this d-d band is increased due to the influence of nearby intense charge-transfer transitions. The other d-d transitions were masked by the strong charge-transfer band [72]. The electronic spectra of transition metal complexes of **45** were also reported

[73]. The spectrum of ligand shows two strong bands at 235 and 385 nm assigned to π–π^* transitions. For all the complexes, the π–π^* bands are not altered to a greater extent on coordination. The spectrum of the Mn(II) complex shows three shoulders at 600, 439, and 360 nm assigned to $^6A_{1g} \rightarrow {}^4T_1$, $^6A_{1g} \rightarrow {}^4T_2(G)$, and $^6A_{1g} \rightarrow {}^4T_2(D)$ transitions, respectively. The electronic spectrum of Fe(III) complex shows a weak broad band in the near IR region at 1451 nm, indicating a square-pyramidal structure. The charge transfer band at 345 nm obscures the rest of the d-d transitions. For the Ni(II) complex, the band at 573 nm is due to $^3A_{2g} \rightarrow {}^3T_{1g}$ transition of Ni(II) in octahedral environment. The spectrum of Cu(II) complex shows two bands at 450 and 627 nm assignable to $^2B_{1g} \rightarrow {}^2A_{1g}$ and $^2B_{1g} \rightarrow {}^2E_g$ transitions, respectively, indicating square planar geometry of the Cu(II) complex.

Kurdekar *et al.* [79] reported electronic spectra of **49**, **50,** and their metal complexes in DMF. The ligands exhibit strong absorptions at 275–292 nm due to inter-ligand transitions. These bands are almost unchanged in spectra of complexes. Absorptions at 350–370 nm attributed to the n–π^* transition associated with azomethine red shift on complexation, indicating coordination of azomethine nitrogen. In the electronic spectrum of Co(II), bands at 465–434 nm are assigned for ligand-to-metal charge transfer (LMCT) transitions. A broad distinct peak at 550 nm assigned to $^4T_{1g} \rightarrow {}^4A_{2g}$ suggests octahedral structure for the complexes. Both Ni(II) complexes have LMCT transitions at 423 nm and d-d transitions around 600 nm assigned to $^3A_{2g} \rightarrow {}^3T_{1g}$, indicating octahedral geometry. Electronic spectra of Cu(II) complexes exhibit a broad intense peak at 445 nm assigned to S → Cu(II) LMCT. Zn(II) complexes show strong absorptions at 370–390 nm for charge transfer.

Electronic spectra of **54**, **55** and their complexes were reported [82]. Both ligands exhibited similar electronic transitions with strong bands at 230–260 nm, assigned to inter-ligand π–π^* transitions. The transitions at 275–300 and 350 nm were assigned to n–π^* transitions of carbonyl and imine, respectively; these peaks undergo red shift on complexation. In all complexes, an intense peak at 400–420 nm was assigned to ligand-to-metal CT transition (S → M). The Co(II) complexes show absorptions at 450, 570, and 830 nm, assigned to d-d transitions. In Ni(II) complexes, the lowest band at 860 nm was due to $^3A_{2g} \rightarrow {}^3T_{2g}$ and bands near 600 and 520 nm were assigned to $^3A_{2g} \rightarrow {}^3T_{1g}$ and $^3A_{2g} \rightarrow {}^3T_{1g}(P)$, respectively. These spin-allowed d-d bands indicate octahedral geometry around Ni(II). Both Cu(II) complexes displayed absorptions at 500 and 550 nm, attributed to d-d transitions of the d^9 system. Zn(II) complexes show only absorptions around 420 nm corresponding to inter-ligand transitions.

Electronic spectra of complexes of Co(II), Ni(II), and Cu(II) with **56** were reported by Kumar *et al.* [83]. The Co(II) and Ni(II) complexes show octahedral geometry and Cu(II) complex exhibits distorted octahedral geometry. The UV–Vis spectra of **57** and its complexes were reported [84]. The bands observed above 351 nm are identical and assigned to π–π^* transitions and inter-ligand charge transfer transitions of the quinoxaline ring, imidazole ring, and azomethine C=N. The n–π^* transition is forbidden and not observed. The spectral studies reveal tetrahedral geometry for Mn(II) complex, octahedral for Fe(III) and Ni(II) complexes, tetrahedral for Co(II), and square planar for Cu(II) complex.

5.3. *^{1}H NMR*

The ^{1}H NMR spectrum of Zn(II) complex of **45** was reported [73]. The disappearance of phenolic OH at 9.70 ppm in the spectrum of Zn(II) complex indicates participation of the phenol in chelation through proton displacement. The signal due to azomethine proton was

shifted upon complexation. The shift of azomethine signal may be due to donation of the lone pair of electrons by nitrogen to zinc. The aromatic and quinoxaline protons resonate as a complex multiplet at 7.46–8.20 ppm. The broad singlet at 3.91–4.26 ppm indicates the presence of water in the coordination sphere.

The ^{1}H NMR spectra of **48** and its Zn(II) complex were reported [78]. The Schiff base exhibits a doublet at 7.16 ppm assigned for the thiazolidine proton resonance. The multiplet at 7.4–8.3 ppm is assigned for two NH protons and for aromatic protons. The azomethine proton appears as a singlet at 8.93 ppm. The multiplets at 7.0–7.9 ppm were assigned for aromatic protons. The spectral data thus confirm ring opening in the presence of metal ion.

The ^{1}H NMR spectra of Zn(II) complexes of hydrazones, **49** and **50,** were reported [79]. The peak at 8.62 ppm for L^1 assigned as azomethine proton, which on complexation shifted downfield, confirms coordination of azomethine nitrogen. Quinoxaline ring –NH resonates at 11.62 and 10.64 ppm for L^1 and L^2, respectively. The aromatic protons give multiplets at 6.93–7.91 ppm. The Zn(II) complexes show small shifts in proton resonance frequencies.

Kulkarni *et al.* [80] reported ^{1}H NMR spectra of a bicompartmental ligand and its Zn (II) complex. In spectra of the complex, the peak at 4.61 ppm is absent and a new broad peak at 11.50 ppm suggests the thio–keto form and sulfur coordination. The peak observed for phenolic OH at 8.40 ppm disappears on complex formation indicating deprotonation and phenoxide coordination. The methylene amine protons show peaks at 3.6 ppm and shift downfield in the complex.

The ^{1}H NMR spectra of **54**, **55** and their Zn(II) complexes were reported [82]. **54** displayed two singlets (D_2O) exchangeable at 11.9 and 11.02 ppm assigned to isatin and quinoxaline ring NH, respectively. They shift upon complexation (to 12.13 and 10.99 ppm), suggesting coordination of oxygen and sulfur through ketone and thione, respectively. Hydrazine NH at 8.53 ppm shifts downfield in the respective Zn(II) complex (9.01 ppm). The aromatic protons resonate at 6.61–7.58 ppm and undergo a little alteration in chemical shift value (6.80–8.04 ppm). Coordinated water resonates at 3.50 ppm and broadens the DMSO peak. In **55**, singlets at 13.52 and 11.88 ppm were ascribed to ring NH of quinoxaline-2,3(1,4H)-dione and hydrazinylquinoxaline-2-thione, respectively. In the Zn(II) complex, they shift downfield (13.82 and 12.18 ppm) due to variation in electron density and steric constraints brought about by chelation. The hydrazine protons resonate at 9.50 ppm as a doublet. In the Zn(II) complex of **55**, due to participation of NH in coordination, the coordinated NH shifts upfield at 10.00 ppm as a doublet. Non-coordinated NH resonates at 8.99 ppm. The aromatic protons (7.08–8.13 ppm) undergo a little change in chemical shifts upon complexation (6.91–8.05 ppm) and coordinated water resonates at 3.50 ppm.

Sebastian *et al.* [84] reported the ^{1}H NMR spectrum of the Zn(II) complex of **57**. The histidine NH proton resonates at 8.4 ppm. A water proton appears as a broad signal at 3.9–4.3 ppm and the aromatic protons are a multiplet at 7.60–8.50 ppm. The azomethine C–H proton gives a singlet at 9.45 ppm. Signals at 6.80–7.00 and 2.08 ppm can be attributed to imidazole and acetate protons, respectively.

Kulkarni *et al.* reported [85] the NMR signal of **58** at 11.91 ppm disappeared on complexation with Zn(II), indicating enolization and coordination of oxygen *via* deprotonation. The signal of the hydrazine NH at 8.89 ppm in the ligand disappeared on complexation due to thioenolization. Sulfur coordination through deprotonation was confirmed by the ^{1}H NMR spectrum. On complexation, signals for amine protons shift from 7.98 to 4.97 ppm and water coordination is shown by the broad peak at 3.70 ppm. Aromatic protons show

small shifts in the spectrum of complex. The Zn(II) complex of **59** was reported. Sharp singlets at 10.29, 9.81, 9.0, and 8.03 ppm were assigned for the ring NH, hydrazine NH, and amine NH protons, respectively. The peaks at 10.29 and 9 ppm disappeared. The spectrum confirms coordination of oxygen and sulfur through deprotonation. The coordinated water protons resonate at 3.50 ppm.

5.4. *EPR*

The EPR spectrum of the Cu(II) complex of **15** at liquid nitrogen temperature (LNT) [51] indicates polycrystalline complex. Four weak signals on the left side of the intense peak correspond to hyperfine resolution of the parallel component. The intense peak corresponding to the perpendicular component of the g tensor, $g_{\|}$, g, g_{iso}, and $A_{\|}$ was evaluated as 2.25, 2.07, 2.16, and 145.36 G, respectively. The observed values show that the ligand does not affect paramagnetic behavior of the Cu(II) complex and suggest tetragonally elongated octahedral environment around Cu(II). The EPR spectrum of Cu(II) complex of **16** gave g_{xx}, g_{yy}, g_{zz}, and g_{av} values as 2.063, 2.088, 2.145, and 2.099, respectively. The g tensor of this complex exhibits nearly rhombic symmetry, suggesting square planar geometry for the complex.

The EPR spectrum of [Cu(QAP$_2$)] was recorded [54] in ethanol at LNT. Three g values were observed for Cu(II) complex, assigned due to distortion from the tetrahedral structure. The EPR spectra of Cu(II) complexes of **26** and **27** were reported [55]. The g and A values obtained from the EPR spectrum of [Cu(QSC)Cl$_2$] in DMSO at LNT indicate that unpaired electron is in the $d_x^2 - d_y^2$ orbital of Cu(II) and the spectral features are characteristics of axial symmetry. The α^2 value reveals covalent metal–ligand bonding. The EPR spectrum of [Cu(QFA)Cl$_2$] in methanol at LNT was obtained. The g and A values indicate axial symmetry for the complex. The α^2 value of the complex supports the covalent nature of the complex.

The EPR spectra of complexes of **32** were reported [57]. The two g values, $g_{\|} = 2.70$ and $g_{\perp} = 2.02$, for Co(II)-PSHQAD indicate square-pyramidal geometry. The Ni(II) complex gives g value at 2.023 indicating octahedral structure of the complex. The Cu(II) complex gives two g values, $g_{\|} = 2.26$ and $g_{\perp} = 2.06$. The spectra reveal strong field ligand. The α^2 values support the covalent nature of metal–ligand bond.

All Ru(III) complexes of **25**, **29,** and **37** were EPR active, suggesting that in all complexes, Ru is in +3 state. The g values observed for Ru(III) complexes of qab and qpd suggest rhombohedral distortion of octahedral geometry. The g values for Ru(III) complexes of qap suggest distorted octahedral geometry of the axial complex [64].

Lakshmi *et al.* [66] reported the EPR spectrum of the Cu(II) complex of **38**. The observed g values suggest nearly rhombic symmetry for the complex. The EPR spectrum of the Cu(II) complex of the Schiff base obtained by condensation of 3-hydroxyquinoxaline-2-carboxaldehyde with 2-mercaptoaniline was reported [70].

The X-band EPR spectrum of the Cu(II) complex of **45** was reported [73]. The spectrum with $g_{\|}$ and $g_{\perp}$ values at 2.28 and 2.12, respectively, was observed. From the spectrum, the unpaired electron is localized in the $d_x^2 - d_y^2$ orbital of Cu(II) and the complex has axial symmetry. The spectrum recorded in DMF at 77 K indicates axial features, suggesting a $d_x^2 - d_y^2$ ground state and square planar geometry around Cu(II). Kurdekar *et al.* [79] reported the solid-state X-band spectra of **49** and **50**. Absence of half field absorption indicates there is no metal-metal interaction.

In solid-state X-band EPR spectra of the Cu(II) complexes of **54** and **55** [82], the complexes exhibit isotropic intense broad signals with g_{iso} of 2.09 and 2.05. No hyperfine splitting in $g_{\|}$ and $g_{\perp}$ or half-field absorptions was observed. The higher covalency of sulfur–metal bond and the lower spin-orbit coupling may be the main factors affecting the EPR spectrum.

X-band EPR spectra of the Mn(II) and Cu(II) complexes of **57** were reported [84]. The Cu(II) complex in polycrystalline state gives a broad signal with a g value of 2.11, due to the dipolar interactions and enhanced spin lattice relaxation. The EPR spectrum of Mn(II) complex at 77 K gives six lines with a g value 2.07. The EPR spectrum of the Cu(II) complex in DMF at 77 K exhibits two $g_{\|}$ values and one $g_{\perp}$ value, suggesting Cu(II) in two different environments. The axial spectrum of Cu(II) complex at 77 K reveals that the unpaired electron is localized in the $d_x^2 - d_y^2$ orbital. At 298 K, EPR spectrum of the Cu (II) complex is isotropic irrespective of solvent with four well-resolved lines. Kulkarni *et al.* [85] reported that EPR spectra of Cu(II) complexes $[CuL^1(H_2O)]$ and $[CuL^2(H_2O)]$ exhibit isotropic intense broad signals with g_{iso} values 2.09 and 2.05, respectively.

The EPR spectrum of $[VO(HQO)_2]$ was reported [88]. The complex spectrum clearly shows both $g_{\|}$ and $g_{\perp}$ components with axially symmetric g tensor and hyperfine coupling (A) tensor. The Δg values are unusually low and g_{iso}(1.999) is close to the free-electron g value, indicating the complex must have unpaired electron loosely bound to the metal.

5.5. *Cyclic voltammetry*

Cyclic voltammetry is the most useful electro-analytical technique for study of electrochemical properties of metallo-organic species. Important parameters of cyclic voltammograms are the magnitudes of the peak current (I_{pa}, I_{pc}) and peak potential (E_{pa}, E_{pc}).

Arun *et al.* [74] reported the cyclic voltammetry study of **43**c. Cyclic voltammogram of **43** displayed a quasi-reversible redox process with a peak-to-peak separation of 203 mV. The ligand is susceptible to easy oxidation and reduction. Cyclic voltammogram of the Ru (II) complex shows two quasi-reversible redox processes occurring at negative potential and with a peak-to-peak separation of 182 and 209 mV, respectively, suggesting ligand-centered process. Due to this, the peak potentials for Ru(II)/Ru(III) couple shift to more negative potential.

Kurdekar *et al.* [79] reported the cyclic voltammograms of mononuclear transition metal complexes with bi and tridentate **49** and **50** with a quinoxaline moiety. Electrochemical properties of two ligands and their metal complexes were studied from 1.2 to −1.6 V. Cyclic voltammograms of Cu(II) complexes of both ligands show well-defined redox processes corresponding to the Cu(II)/Cu(I) couple. Both Cu(II) complexes show quasi-reversible redox process with one electron transfer. Cyclic voltammetry of some binuclear quinoxaline-based Schiff base complexes was reported [80].

Kulkarni *et al.* [82] reported cyclic voltammetric studies of **54**, **55** and their metal complexes. The Cu(II) and Ni(II) complexes only show redox reactions in the applied potential range.

5.6. *Thermal studies*

The thermal studies are in agreement with IR and elemental analysis for the presence of water. Lattice water is lost at lower temperature than coordinated water. After elimination of coordinated water, decomposition of the ligand occurs.

Thermal behavior of complexes of Fe(III), Co(II), Ni(II), and Cu(II) of **11** were reported [46]. All the complexes are stable to 120 °C and show two DTG peaks. The first DTG peak occurs at 293 °C for the Fe(III) complex, 330 °C for the Co(II) and Ni(II) complexes, and 228 °C for the Cu(II) complex. The mass-loss data for this stage correspond to the loss of two waters, four hydroxyl groups and one chlorine for the Fe(III) complex and four waters, two hydroxyl groups and one chlorine for the other complexes. The TG studies thus agree with the conclusion from IR studies and elemental analysis for the presence of water and hydroxyl groups. A second DTG peak is at 670 °C for the Fe(III) complex, 518 °C for the Co(II) complex, 534 °C for the Ni(II) complex, and 645 °C for the Cu(II) complex. Mass-loss data suggest that the Schiff base ligand has been expelled during this stage. The product at the end of the decomposition in all the cases was metal oxides.

Thermal analysis of complexes of **32** was reported [57]. Up to 110 °C, the complexes are stable. Decomposition takes place in two steps; in the first step below 100 °C there is a small decrease in weight due to loss of physisorbed water. In the second-stage decomposition, 40% weight loss occurs. The decomposition completes at 600 °C.

Chittilapilly and Yusuff [64] reported the thermal properties of Ru(III) complex of Schiff base derived from 3-hydroxyquinoxaline-2-carboxaldehyde. The complex exhibits three steps of decomposition. Mass loss at 50–100 °C was assigned for loss of lattice water. Decomposition from 120–170 °C is due to removal of coordinated water. The final decomposition above 280 °C was due to decomposition of ligands.

TG/DTG curves of encapsulated complexes of **25**, **29,** and **37** show that the decomposition pattern is same for all complexes. DSC curve gives an endothermic peak corresponding to deaquation of the sample at 100 °C and an exothermic maximum corresponding to decomposition of the encapsulated complexes [65].

Lakshmi *et al.* reported the absence of coordinated water in metal complexes of **38** by using TGA and DTA [65]. Sebastian *et al.* [72] reported the thermal properties of a Co(II) complex of **45**. The mass loss at 50–120 °C corresponds to loss of one water. The organic part of the complexes decomposes in two steps. The first shows 39% mass loss at 343 °C with a DTA endotherm at 348 °C, corresponding to loss of two 2-amino-5-methylphenol parts of the two Schiff bases. The second stage of decomposition starts at 412 °C and is continuous, corresponding to removal of quinoxaline. The decomposition was not complete even at 800 °C.

Thermal stability of Mn(II), Co(II), Ni(II), Cu(II), and Zn(II) complexes of **45** was also investigated using TG-DTA studies under nitrogen with heating rate of 10 °C min^{-1} over a temperature range of 40–1000 °C. The Schiff base exhibits single-stage decomposition above 160 °C. Loss of lattice water in Mn(II), Ni(II), and Zn(II) complexes was observed below 200 °C. All the complexes were thermally stable and show multi-stage decomposition. The organic part in all the complexes decomposes above 200 °C [73].

Arun *et al.* [75] reported TG and DTA analysis of Ru(III) complex of **43**. The mass loss to 85 °C corresponds to loss of lattice water. The removal of coordinated chlorine occurs at 240–280 °C. Above 280 °C, the ligand starts to decompose and was not complete even after 1000 °C. Similarly, the Ni(II) complex of the same ligand was also subjected to TG and DTA thermal studies. The loss of lattice water occurs at 40–130 °C. Coordinated water is lost at 130–250 °C. Above 250 °C, the ligand starts to decompose and decomposition was not complete even above 1000 °C.

The thermal stability of **48** and its complexes was reported by Sebastian *et al.* [78]. The weight loss observed for the Co(II) complex from 90–120 °C indicates the presence of

three lattice waters. Weight loss at 150–200 °C for the Mn(II), Co(II), and Ni(II) complexes can be attributed to loss of coordinated water.

Kulkarni *et al.* [80] reported thermal studies of **51** and its metal complexes. The Ni(II) and Cu(II) complexes show a plateau region up to 230 °C, indicating absence of water in the complex. Decomposition at 230–290 °C with weight loss (15.81%) was assigned for removal of three chlorines as HCl. Metal oxides were obtained as the final product.

The thermal analysis of transition metal complexes of **57** was reported [84]. In all complexes, weight loss below 120 °C was assigned to loss of lattice water. The presence of coordinated water in Ni(II) and Fe(III) complexes was confirmed by weight loss at 140–210 °C. All the complexes are thermally stable and exhibit multi-stage decomposition.

Kulkarni *et al.* [85] reported that Cu(II) complexes of **58** and **59** decompose with two steps. The first corresponds to loss of coordinated water. The ligands decompose from 250 to 380 °C, assigned as the second stage decomposition. The final product was metal oxide.

5.7. *X-ray crystallography*

Crystallographic study of Co(II) Schiff base complex obtained from **45** has been reported by Sebastian *et al.* [72]. The Co(II) coordination sphere is distorted octahedrally with a *cis* arrangement of N_4O_2 donors of two tridentate NNO Schiff bases. The molecules exhibit a 2-D polymeric structure parallel to the [1 0 1] plane formed by O–H…N and O–H…O intermolecular hydrogen bonds and π–π stacking. The crystal is a racemic mixture of two crystallographically independent enantiomers of the complex. They also reported [73] the crystal structure of Ni(II) complex of **45**. The crystal structure is a racemic mixture of crystallographically independent enantiomers of the complex. The molecule exhibits a [0 1 0] plane, formed by O–H…N and O–H…O intermolecular hydrogen bonds and π–π stacking.

6. Biological applications

6.1. *Antibacterial and antifungal activity*

Chittilapilly *et al.* [64] screened **25**, **29**, **37** and their Ru(III) complexes for antibacterial activity. The metal complexes exhibit considerable inhibitory action. The inhibition increased with increase in concentration of complexes.

Lakshmi *et al.* [71] reported the bactericidal properties of **44** and its metal complexes. The studies indicate promising activity against *S. aureus*. The antimicrobial activity of **58** and its Co(II), Ni(II), and Cu(II) complexes has been tested by disk diffusion technique [83]. The results show that the metal complexes are more active than AQTC. The Schiff bases (**15**, **16**, **38,** and **44**) and their VO (IV) complexes were evaluated for antimicrobial activity against gram-positive and gram-negative bacteria. Some complexes were more active than the ligand. In some cases, ligands and their complexes have similar activity against bacteria [88].

6.2. *Antidiabetic activity*

Antidiabetic activities of quinoxaline Schiff bases **58**, **59** and their Zn(II) complexes in the diabetes-induced Wister rats were reported [85]. Evaluation of antidiabetic activity was done by blood glucose test and oral glucose tolerance test. [Zn(**58**)(H_2O)] and **59** have showed notable reduction of blood glucose level.

7. Conclusion

The "Quinoxaline-based Schiff base transition metal complexes: Review" was chosen based on the urgent need to find compounds that can be more effective and less toxic therapeutic substitutes for existing antimalarial drugs. An attempt has been made to present salient facts relative to the importance of quinoxaline in various treatments. The material collected in the review shows quinoxaline as a biologically important system. The general summary of quinoxaline chemistry might be that fundamental reactions of quinoxaline are well understood, but that many other quinoxaline reactions are not well developed. Hopefully, this review will make some of the unexplored areas of quinoxaline more apparent, and will encourage further development of the unexplored areas, stimulating new ideas for quinoxaline chemistry.

Future outlook

The quinoxaline system is very active biologically. Because of the increase in antimicrobial resistance to drugs, it is worthwhile to synthesize compounds with less side effects and more biological activity. A goal of present-day inorganic coordination chemists and pharmacological investigations is discovery and development of better drugs to fight diseases. This has led to numerous studies on drug–metal complexes [89]. Quinoxaline is part of various antibiotics, such as levomycin, echinomycin, and actinoleutin, known to inhibit growth of gram-positive bacteria [90] and active against various transplantable tumors.

Abbreviations

QCG	Schiff base derived from quinoxaline-2-carboxaldehyde and glycine
H-QTSC	quinoxaline-2-carboxaldehyde thiosemicarbazone
H_2BSDHQ	bis(N-salicylidene)-2-3-dihydrazino-1,4-quinoxaline
HSHQO	N-salicylidene-3-hydrazinoquinoxaline-2-one
HHAHQO	N-(2-hydroxy)acetophenoyl-3-hydrazinoquinoxaline-2-one
BHQ	2,3-bishydrazinoquinoxaline
QHA	3-hydroxy quinoxaline-2-carboxalidene-o-aminophenol
QHS	3-hydroxyquinoxaline-2-carboxaldehydesemicarbazone
QHF	3-hydroxyquinoxaline-2-carboxalidene furfurylamine
QHT	3-hydroxyquinoxaline-2-carboxaldehydethiosemicarbazone
QAP	deprotonated quinoxaline-2-carboxalidene-2-aminophenol
QSC	Schiff base derived from quinoxaline-2-carboxalidene and semicarbazide
QFA	Schiff base derived from quinoxaline-2-carboxalidene and furfurylamine
QED	N,N′-bis(3-hydroxyquinoxaline-2-carboxalidene)ethylenediamine
QPD	N,N′-bis(3-hydroxyquinoxaline-2-carboxalidene)o-phenylenediamine
QHD	3-hydroxy quinoxaline-2-carboxaldehydehydrazone
QAB	Schiff base derived from 3-hydroxyquinoxaline-2-carboxaldehyde and 2-aminobenzimidazole
QDT	N,N′-bis(3-hydroxyquinoxaline-2-carboxalidene)diethylenetriamine
PS-HQAD	polymer anchored Schiff base
QXDO	2,3-quinoxalinedioxime
BQXDP	N,N′-bis(3-quinoxaline-2-one)diamino propane
NBHQO	N-(2-nitro)-benzilidene-3-hydrazinoquinoxaline-2-one
HQCDMN-H_2	N,N′-bis(3-hydroxyquinoxaline-2-carboxalidene)2,3-diaminomaleo nitrile
HQCDAN-H_2	N,N′-bis(3-hydroxyquinoxaline-2-carboxalidene)1,8-diamino naphthalene
HQCDAC-H_2	N,N′-bis(3-hydroxyquinoxaline-2-carboxalidene)trans (R,R′)1,2-diaminocyclohexane

HQCAP-H_2	3-hydrazinoquinoxaline-2-carboxali dene-2-aminophenol
HQCAAP-H_2	3-hydroxyquinoxaline-2-carboxalidene-4-aminoantipyrine
HDHAHQO	Schiff base derived from 3-hydrazinoquinoxaline-2-one and dehydroacetic acid
HQO	3-hydrazino quinoxaline-2-one
DHA	dehydro aceticacid
AQSC	Schiff base derived from 2-aroylquinoxalinesemicarbazone
BTQ	3-(2,3-dihydro-1,3-benzothiazol-2-yl)quinoxaline-2(1H)-one
AQTC	2-phenylquin oxalinethiosemicarbazone
QLH	Schiff base derived from quinoxaline-2-carboxali dene and L-histidine
H_2BSDHQ	bis(N-salicylidene)-2-3-dihydrazino-1,4-quinoxaline

Acknowledgments

We are thankful to Council of Scientific and Industrial Research (CSIR), New Delhi, India, for the financial support in the form of a research project (Scheme No: 01(2453)/11/EMR-II).

References

[1] H. Schiff. *Ann. Suppl.*, **3**, 343 (1864).
[2] C.J. Dhanaraj, M.S. Nair. *J. Coord. Chem.*, **62**, 4018 (2009).
[3] M.S. Nair, R.S. Joseyphus. *Spectrochimica Acta, Part A: Molecular and Biomolecular Spectroscopy*, **70**, 794 (2008).
[4] H. Keypour, M. Shayestheh, R. Golbedaghi, A. Chehregani, A.G. Blackman. *Journal of Coordination Chemistry*, **65**, 1004 (2012).
[5] N. Raman, J. Joseph, S.M. Kumar, K. Sahayaraj. *J. Biopesticides*, **1**, 206 (2008).
[6] B.S. Creaven, M. Devereux, D. Karcz, A. Kellett, M. McCann, A. Noble, M. Walsh. *Journal of Inorganic Biochemistry*, **103**, 1196 (2009).
[7] S. Kumar, N.D. Dhar, N.P. Saxena. *J. Sci. Indian Res.*, **68**, 181 (2009).
[8] A. Majumder, G.M. Rosair, A. Mallick, N. Chattopadhya, S. Mitra. *Polyhedron*, **25**, 1753 (2006).
[9] W. Zhang, J.L. Loebach, S.R. Wilson, E.N. Jacobsen. *Journal of the American Chemical Society*, **112**, 2801 (1990).
[10] R. Irie, K. Noda, Y. Ito, N. Matsumoto, T. Katsuki. *Tetrahedron Letters*, **31**, 7345 (1990).
[11] M.G. Bhowon, H.L.K. Wah, R. Narain. *Polyhedron*, **18**, 341 (1999).
[12] G. Xie, T. Li, A. Zhang. *Inorganic Chemistry Communications*, **13**, 1199 (2010).
[13] R.G. Cavell, K. Aparna, R.P.K. Babu, Q. Wang. *Journal of Molecular Catalysis A: Chemical*, **189**, 137 (2002).
[14] I. Ronconi, P.J. Sadler. *Coordination Chemistry Reviews*, **251**, 1633 (2007).
[15] C.W. Tang, S.A. VanSlyke. *Applied Physics Letters*, **51**, 913 (1987).
[16] P.G. Lacroix, S.D. Bella, I. Ledoux. *Chemistry of Materials*, **8**, 541 (1996).
[17] E.J. Martina, C. Holzer, M. Volpe, N.C. Mosch-Zanetti. *Inorganic Chemistry*, **51**, 9956 (2012).
[18] M.H. Torre, D. Gambino, J. Araujo, H. Cerecetto, M. Gonzalez, M.L. Lavaggi, A. Azqueta, A.L. De Cerain, A.M. Vega, U. Abram, A.J. Costa-Filho. *European Journal of Medicinal Chemistry*, **40**, 473 (2005).
[19] Y.B. Kim, Y.H. Kim, J.Y. Park, S.K. Kim. *Bioorganic & Medicinal Chemistry Letters*, **14**, 541 (2004).
[20] D. Schenfelder, D. Slumm, G. Bhola, N. Niclas. *J. Pharm.*, **43**, 837 (1998).
[21] F.F. Paul, S.A. Lang, L. Yang, T. Cufcik. *Journal of Medicinal Chemistry*, **72**, 973 (1960).
[22] K. Sasse, H.R. Wegler, G. Unterstenhofer, F. Grewe. *Angewandte Chemie*, **72**, 973 (1960).
[23] M.S. Refat, I.M. El-Deen, Z.M. Anwer, S. El-Ghol. *Journal of Coordination Chemistry*, **62**, 1709 (2009).
[24] P.H. Wang, G.J. Keck, E.J. Lien, M.M.C. Lai. *Journal of Medicinal Chemistry*, **33**, 608 (1990).
[25] J. Ziegler, T. Shurela, L. Pasierb, C. Kelly, A. Elamin, K.A. Cole, D.W. Wright. *Inorganic Chemistry*, **39**, 373 (2000).
[26] X. He, C.Z. Lu, C.D. Wu. *Journal of Coordination Chemistry*, **59**, 977 (2006).
[27] T. Yamato, K. Sugiyama, T. Kushida, T. Inoue, T. Kanbara. *Journal of the American Chemical Society*, **118**, 3930 (1996).
[28] Y. Cui, X. Zhang, S.A. Jenekhe. *Macromolecules*, **32**, 3824 (1999).
[29] W. Blau. *Physics in Technology*, **18**, 250 (1987).

[30] H.W. Yoo, M.E. Suh, S.W. Park. *Journal of Medicinal Chemistry*, **11**, 4716 (1998).
[31] C.J. Hwa, J.J. Ok, C.J. Mi, H.Y. Sung, C.K. Ryu, C. Hoe-Kwang, L. Kook. *Biorg. Med. Chem. Lett.*, **15**, 3380 (2005).
[32] B. Asha, B.R. Abdul, A. Amir. *European Journal of Medicinal Chemistry*, **44**, 1317 (2009).
[33] R. Sastry, C.V. Marwah, P. Marwah, G. Rao. *Indian J. Chem.*, **28B**, 885 (1989).
[34] J.J. Li. *Journal of Organic Chemistry*, **64**, 8425 (1999).
[35] Y. Deepika, P.S. Nath, K. Sachin, S. Shewtha. *IJCPR*, 1 (2011).
[36] Y.A. Ammar, M.S.A. El-Gaby, M.A. Zahran, A.A. Abdel-Salam. *Phosphorus Sulfur Silicon and the Related Elements*, **157**, 87 (2000).
[37] D. Varghese, V. Arun, M. Sebastian, P. Leeju, G. Varsha, K.K.M. Yusuff. *Acta Crystallogr., Sect. E*, **65**, 435 (2009).
[38] D. Vargheese, V. Arun, P.P. Robinson, M. Sebastian, P. Leeju, G. Varsha, K.K.M. Yusuff. *Acta Crystallogr., Sect. C*, **65**, 612 (2009).
[39] V. Arun, P.P. Robinson, S. Manju, P. Leeju, G. Varsha, V. Digna, K.K.M. Yusuff. *Dyes and Pigments*, **82**, 268 (2009).
[40] P. Leeju, V. Arun, M. Sebastian, G. Varsha, D. Vargheese, K.K.M. Yusuff. *Acta Crystallogr., Sect. E*, **65**, 1981 (2009).
[41] V.G. Ratnadeep, J.S. Pramodkumar. *IJPRD*, **3**, 157 (2011).
[42] V.G. Ratnadeep, J.S. Pramodkumar. *Bangladesh J. Pharmacol.*, **6**, 92 (2011).
[43] V.G. Ratnadeep, J.S. Pramodkumar. *Int. J. Exp. Pharmacol.*, **2**, 44 (2012).
[44] X. Zhengfeng, Z. Jainzhong, L. Fangming. *Chin. J. Org. Chem.*, **31**, 548 (2011).
[45] L. Achutha, M. Deepthi, B.M. Reddy, A. Ravikiran, V.H. Babu. Inventi. Rapid: Med. Chem., Inventi:pmc/133/11 (2012).
[46] K.K.M. Yusuff, R. Sreekala. *Synthesis and Reactivity in Inorganic and Metal-Organic Chemistry*, **21**, 4 (1991).
[47] R. Sreekala, K.K.M. Yusuff. *Reaction Kinetics and Catalysis Letters*, **48**, 575 (1992).
[48] A.R. Karthikeyan. Studies on some new complexes of iron, cobalt, nickel and copper. PhD thesis, Cochin University of Science and Technology (1992).
[49] R. Sreekala, K.K.M. Yusuff. *Synthesis and Reactivity in Inorganic and Metal-Organic Chemistry*, **24**, 10 (1994).
[50] D.S. Rani, P.V.A. Lakshmi, V. Jayatyagaraju. *Transition Metal Chemistry*, **19**, 75 (1994).
[51] P.V.A. Lakshmi, D.S. Rani, V. Jayatyagaraju. *Asian Journal of Chemistry*, **7**, 296 (1995).
[52] J. Mathew. Synthesis, characterization and catalytic activity studies of some new transition metal chelates of the Schiff bases derived from 3-hydroxy quinoxaline-2-carboxaldehyde. PhD thesis, Cochin University of Science and Technology (1995).
[53] S.G. Valavi. Studies on some new metal complexes of quinoxaline based ligands. PhD thesis, Cochin University of Science and Technology (1996).
[54] S. Mayadevi, K.K.M. Yusuff. *Synthesis and Reactivity in Inorganic and Metal-Organic Chemistry*, **27**, 319 (1997).
[55] S. Mayadevi, P.G. Prasad, K.K.M. Yusuff. *Synthesis and Reactivity in Inorganic and Metal-Organic Chemistry*, **33**, 481 (2003).
[56] N.R. Suja. Studies on Some Supported Co(II), Ni(II) and Cu(II) Complexes of o-Phenylenediamine and Schiff bases Derived from 3-Hydroxyquinoxaline-2-carboxaldehyde. PhD thesis, Cochin, University of Science and Technology (2002).
[57] N.R. Suja, K.K.M. Yusuff. *Journal of Applied Polymer Science*, **91**, 3710 (2004).
[58] L. Wang, X.J. Zhu, W.Y. Wong, J.P. Guo, W.K. Wong, Z.Y. Li. *Dalton Transactions*, **19**, 3235 (2005).
[59] L. Wang, W.K. Wong, L. Wu, Z.Y. Li. *Chemistry Letters*, **34**, 934 (2005).
[60] Y.B. Dong, H.Q. Zhang, J.P. Ma, R.Q. Huang. *Crystal Growth & Design*, **5**, 1857 (2005).
[61] G. Gamo. Studies on metal complexes derived from physiologically active quinoxaline derivatives. Thesis, Addis Ababa University (2006).
[62] M. Yohannes. Synthesis and characterization of metal complexes of a new heterocyclic ligand. Thesis, Addis Ababa University (2006).
[63] X.Q. Che, L.B. Wang. *Acta Crystallogr., Sect. E*, **63**, 2681 (2007).
[64] X. Wu, A.E.V. Gorden. *Journal of Combinatorial Chemistry*, **9**, 601 (2007).
[65] P.S. Chittilapilly, N. Sridevi, K.K.M. Yusuff. *Journal of Molecular Catalysis A: Chemical*, **286**, 92 (2008).
[66] P.V.A. Lakshmi, P.S.S. Reddy, V.J. Raju. *Bulletin of the Chemical Society of Ethiopia*, **22**, 385 (2008).
[67] P.S. Chittilapilly, K.K.M. Yusuff. *Indian J. Chem.*, **47A**, 848 (2008).
[68] X. Wu. Synthesis and applications of 2-Quinoxalinol salens and their metal complexes. PhD thesis, Auburn University (2008).
[69] A.G. Budie. Heterocyclic multidentate ligand containing triazine and quinoxaline functions and its metal complexes synthesis and structural studies. Thesis, Addis Ababa University (2008).

[70] V. Arun. Synthesis and characterization of new transition metal complexes of Schiff bases derived from 3-hydroxyquinoxaline-2-carboxaldehyde and application of some of these complexes as hydrogenation and oxidation catalysts. PhD thesis, Cochin University of Science and Technology (2009).
[71] P.V.A. Lakshmi, B.S. Shyamala, V.J. Raju. *Polish Journal of Chemistry*, **83**, 1555 (2009).
[72] M. Sebastian, V. Arun, P.P. Robinson, P. Leeju, D. Varghese, G. Varsha, K.K.M. Yusuff. *Journal of Coordination Chemistry*, **63**, 307 (2010).
[73] M. Sebastian, V. Arun, P.P. Robinson, A.A. Varghese, R. Abraham, E. Suresh, K.K.M. Yusuff. *Polyhedron*, **29**, 3014 (2010).
[74] V. Arun, N. Sridevi, P.P. Robinson, S. Manju, K.K.M. Yusuff. *Journal of Molecular Catalysis A: Chemical*, **304**, 191 (2009).
[75] V. Arun, S. Mathew, P.P. Robinson, M. Jose, V.P.N. Nampoori, K.K.M. Yusuff. *Dyes and Pigments*, **87**, 149 (2010).
[76] S. Budagumpi, N.V. Kulkarni, G.S. Kurdekar, M.P. Sathisha, V.K. Revankar. *European Journal of Medicinal Chemistry*, **45**, 455 (2010).
[77] B.K. Rai. *Asian Journal of Chemistry*, **22**, 2761 (2010).
[78] M. Sebastian, V. Arun, P.P. Robinson, K.K.M. Yusuff. *Synth. Inorg.-Org. Chem. Nano-Met. Chem.*, **40**, 541 (2010).
[79] G.S. Kurdekar, N.V. Kulkarni, S. Budagumpi, M.P. Sathisha, N.H. Bevinhalli, V.K. Revankar. *Journal of Coordination Chemistry*, **63**, 2172 (2010).
[80] N.V. Kulkarni, G.S. Kurdekar, S. Budagumpi, V.K. Revankar. *Journal of Coordination Chemistry*, **63**, 3301 (2010).
[81] Y. Hu, Q. Liq, Q. Guo, N.G. Luy, Y. Liz. *Dalton Transactions*, **39**, 11344 (2010).
[82] N.V. Kulkarni, N.H. Bevinhalli, V.K. Revankar. *Journal of Coordination Chemistry*, **63**, 1785 (2010).
[83] B. Kumar, B.K. Rai, N. Ambastha. *Oriental Journal of Chemistry*, **27**, 1173 (2011).
[84] M. Sebastian, V. Arun, P.P. Robinson, P. Leeju, D. Varghese, G. Varsha, K.K.M. Yusuff. *Journal of Coordination Chemistry*, **64**, 525 (2011).
[85] N.V. Kulkarni, V.K. Revankar, B.N. Kirasur, M.H. Hugar. *Medicinal Chemistry Research*, **21**, 663 (2012).
[86] P.M.V. Kumar, P.K. Radhakrishnan. *Inorganica Chimica Acta*, **375**, 84 (2011).
[87] G. Qian-Ni, C. Zhong, L. Yun-Guo, C. Shi, L. Zao-Ying. *Journal of Inclusion Phenomena and Macrocyclic Chemistry*, **72**, 79 (2012).
[88] P.V.A. Lakshmi, T. Satyanarayana, P.S. Reddy. *Chinese Journal of Chemistry*, **30**, 935 (2012).
[89] N. Wasi, H.B. Singh. *Inorganica Chimica Acta*, **135**, 134 (1987).
[90] A. Dell, D.H. William, H.R. Mowe, G.A. Smith, J. Feeney, G.C.K. Roberts. *Journal of the American Chemical Society*, **7**, 2497 (1975).